photonics

MDPI

*Review*

# Advances in High-Efficiency Blue OLED Materials

**Xiaoxue Yang [1], Ge Mu [1,*], Kangkang Weng [1,2] and Xin Tang [1,2]**

[1] School of Optics and Photonics, Beijing Institute of Technology, Beijing 100081, China; kangkangweng@bit.edu.cn (K.W.); xintang@bit.edu.cn (X.T.)
[2] Yangtze Delta Region Academy, Beijing Institute of Technology, Jiaxing 314019, China
* Correspondence: gemu@bit.edu.cn

**Abstract:** Organic light-emitting diode (OLED) technology has rapidly emerged in the display and lighting sectors due to its high contrast ratio, wide viewing angle, and sleek design. Beyond these attributes, OLEDs have also demonstrated crucial applications in medicine, fashion, sports, and more, leveraging their emissive properties and flexible design. As the cornerstone of full-color displays, blue OLEDs, whose performance directly impacts color rendition and saturation, have garnered significant attention from both scientific researchers and industrial practitioners. Despite the numerous advantages of OLED technology, blue OLEDs still confront formidable challenges in terms of luminous efficiency, durability, and material stability. This review examines the evolution of blue OLED materials over recent years, specifically focusing on three generations: fluorescent, phosphorescent, and thermally activated delayed fluorescence (TADF). Through molecular design, device structure optimization, and the application of innovative technologies, remarkable advancements have been achieved in enhancing the luminous efficiency, lifetime, and color purity of blue OLEDs. However, to advance commercialization, future efforts must not only ensure high efficiency and long lifetime but also improve material stability, environmental sustainability, and reduce development costs. Emerging materials such as thermally activated exciton materials and the application of hyperfluorescent (HF) OLED technology represent vital driving forces for the continuous advancement of blue OLED technology. It is anticipated that significant milestones will continue to be achieved in the development of highly efficient blue OLEDs in the future.

**Keywords:** high efficiency; blue OLED; fluorescent materials; phosphorescent materials; TADF materials

check for updates

**Citation:** Yang, X.; Mu, G.; Weng, K.; Tang, X. Advances in High-Efficiency Blue OLED Materials. *Photonics* **2024**, *11*, 864. https://doi.org/10.3390/photonics11090864

Received: 13 August 2024
Revised: 5 September 2024
Accepted: 11 September 2024
Published: 13 September 2024

## 1. Introduction

Since Tang et al.'s innovative discovery in 1987 [1], organic light-emitting diodes (OLEDs) have rapidly emerged as a pivotal technology in displays and lighting. Unlike traditional LEDs, OLEDs do not require a backlight, which allows for thinner and more flexible displays. This inherent design advantage, combined with a high contrast ratio, wide viewing angle, and superior color accuracy, makes OLEDs particularly beneficial for modern, ultra-slim display devices. Bridging the gap towards smarter lifestyles, OLED technology is transforming our living spaces and visual experiences at an unprecedented pace. Compared to conventional LED technology, OLEDs offer several key benefits, including improved energy efficiency, the ability to produce deeper blacks and brighter colors, and greater design flexibility for both displays and lighting solutions.

Entering the 21st century, the commercialization OLEDs has accelerated, significantly expanding the boundaries of lighting and display technologies. They pose strong competition to traditional liquid crystal display (LCD), conventional light-emitting diode (LED)—specifically, the standard inorganic LEDs commonly used in displays and lighting—as well as vacuum fluorescent display (VFD) technologies. The demand for lighting in all industries is substantial. In the field of global energy consumption, the lighting industry accounts for about 20% of the share and cannot be ignored as a vital and non-negligible component [2]

(p. 1). Lighting accounts for a significant portion of global electricity consumption and greenhouse gas emissions, and it also constitutes a notable share of energy consumption in homes and businesses [3]. Compared to conventional lighting LEDs, such as high-brightness LEDs and standard white LEDs, OLEDs offer several advantages. OLEDs are generally lighter due to their thin, flexible nature, which reduces the weight compared to the often rigid and bulky LED modules. They also consume less energy for the same light output, as OLEDs typically operate at lower voltages and can achieve comparable brightness with higher efficiency. Additionally, OLEDs have a longer operational lifetime, often surpassing that of conventional LEDs in terms of consistent performance over time. Their response times are faster, meaning they can switch on and off more quickly, which is particularly beneficial for applications requiring rapid changes in lighting conditions. Moreover, OLEDs come in a wider variety of forms compared to traditional LEDs. They can be made into flexible, transparent, or even bendable panels, allowing for innovative lighting designs and applications that are not feasible with conventional LEDs [4,5]. Not to be overlooked, OLEDs align with global trends towards energy conservation, emission reduction, and green development, making them increasingly popular for indoor, automotive, and medical lighting applications. Additionally, OLEDs hold immense potential in the production of light-emitting textiles, poised for growth in healthcare, fashion, and sports [6]. In displays, OLED technology, with its distinctive features of self-emissive nature, exceptional color reproduction, wide viewing angles, flexible design potential, and rapid response, has become the mainstream choice for high-end smartphones, TVs, and wearable-device screens [4,7,8]. As a high-resolution, low-latency display solution, OLEDs are vital for emerging technologies such as augmented reality (AR) and virtual reality (VR) [9]. In addition to its familiar applications in display and lighting, OLED technology has begun to make inroads into the biomedical field (Figure 1). Its luminous properties facilitate phototherapy, promoting cell growth and wound healing, while offering new insights into brain function and disease mechanisms [10]. Wearable devices monitor physiological indices like heart rate and blood oxygen saturation, enhancing health management. This trend is pushing towards fully biocompatible OLED technology for implantable medical devices, aiming for long-term stable in vivo treatment and monitoring [10–13]. In the future, OLED technology, with its unique performance advantages and broad application potential, will continue to drive technological progress and improve user experiences across various fields.

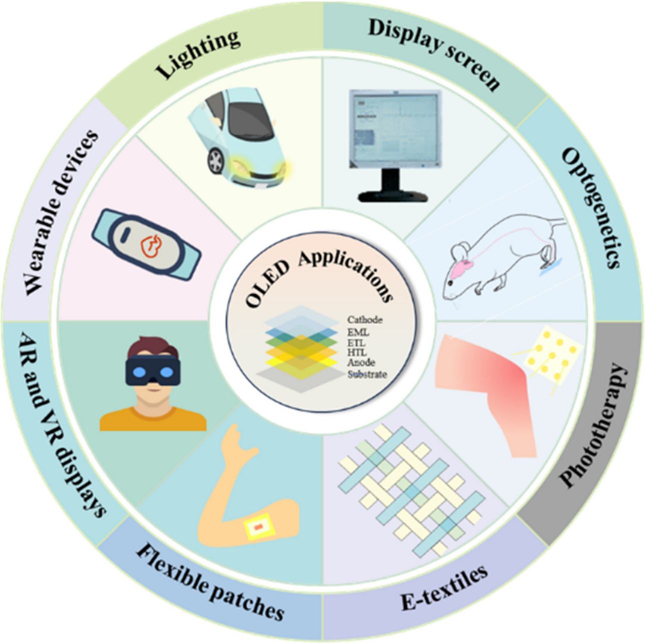

**Figure 1.** OLED technology for applications [6–13].

The pursuit of efficient full-color displays requires advancements in self-emissive RGB pixel materials. Blue emitters play a crucial role in white emission chromaticity for OLED full-color displays [14], directly impacting color reproduction and saturation [15]. As a critical component, their luminous efficiency significantly affects display energy consumption, effectiveness, and user experience, promoting low power usage, long lifetime, and superior display quality. Unlike red and green OLEDs, blue OLEDs have wider full-width-at-half-maximum (FWHM) values in their emission spectra, hindering color purity in high-end electronic displays [16]. Additionally, the production of blue light by blue emitters requires substantial energy input, leading to increased power consumption and heat generation, which ultimately translates to reduced efficiency. The non-radiative dissipation of triplet excitons further restricts the internal quantum efficiency (IQE) of conventional fluorescent devices. Furthermore, to achieve high color purity, as required by ultra-high-definition standards like BT.2020, the standard color coordinate (CIE) for blue light is (0.131, 0.046). However, the scarcity of both pure-blue and deep-blue phosphors, along with compatible host materials, poses a challenge in creating efficient blue OLEDs. While innovative materials such as thermally activated delayed fluorescence (TADF) and triplet–triplet annihilation (TTA) show promising potential in enhancing external quantum efficiency (EQE), the availability of stable and efficient pure-blue and deep-blue emitters is still lacking [7,17–20] (p. 2).

Currently, stable red and green phosphorescent OLED materials are available on the market. These devices, at a brightness of 1000 cd/m$^2$, have an LT$_{50}$ (the time required for brightness to decrease to 50% of its initial value) exceeding 10$^5$ h. However, blue OLED materials still primarily rely on fluorescence technology for commercialization due to the poor stability of blue phosphorescent materials. Although blue phosphorescent materials offer higher efficiency than fluorescence materials, their LT$_{70}$ (the time required for brightness to decrease to 70% of its initial value) is usually less than 100 h at an initial brightness of 1000 cd/m$^2$, making them unsuitable for practical applications. Therefore, there is a need to focus on developing blue OLED materials with both high efficiency and long lifetime [18,21]. The commercialization of blue OLED materials is advancing rapidly, with several companies making significant progress in this field. Universal Display Corporation (UDC) is leading in the development of blue phosphorescent OLED materials, which are expected to significantly enhance the efficiency and performance of OLED displays. Kyulux has also made breakthroughs in fourth-generation hyperfluorescence technology, and its forthcoming blue hyperfluorescence (HF)-emitting materials are expected to surpass current technologies, further improving performance. Additionally, Samsung Display and LG Display from South Korea have made important strides in blue OLED technology. Samsung Display is advancing both blue phosphorescent and next-generation blue fluorescence (TADF and HF) technologies. LG Display has recently developed a blue phosphorescent OLED panel, utilizing a double-stack tandem architecture and blending blue fluorescence with phosphorescent materials to achieve a combination of long lifetime and high efficiency.

By reviewing the recent literature, it is evident that there has been a significant focus on the design of high-efficiency blue OLED materials in recent years. For instance, there are reviews that consolidate information on materials with shared characteristics. In 2022, Santos et al. [22] presented recent advancements and challenges in blue emitters using polymeric materials. In 2023, Xie et al. [16] examined blue fluorescent materials with narrow FWHM properties over the past two decades and categorized them into six narrowband blue emitters. Additionally, there are articles that discuss strategies for designing molecular structures for various materials. In 2023, Li et al. [23] reviewed diverse molecular structures of blue OLED materials, focusing on incorporating different light-emitting groups in luminescent materials to enhance OLED performance. Similarly, Siddiqui et al. [14] underscored the significance of blue OLEDs in applications like lighting and displays, offering a detailed classification and description of fluorescent, phosphorescent, and TADF materials based on their molecular structure. While researchers delve into material molecular structure design, they are also refining device structures, exploring energy transfer mechanisms, and implementing innovative strategies to boost the luminescence efficiency of materials, extend their lifetime, and enhance other key performance metrics. These research directions have gained momentum in recent years, signaling a positive trend in the advancement of blue OLEDs. If all the results of the latest research are organized, we believe it will be helpful for the research in this field.

Therefore, this review focuses on three materials: fluorescent, phosphorescent, and TADF materials for blue emitters. It first introduces the definitions and key performance parameters of the three materials. Then, it reviews the innovative strategies researched in the last five years to overcome the bottleneck of blue OLED technology, presents the results of the current technological progress and the key challenges, and discusses the potential and development direction of novel materials. We anticipate that this review will serve as a valuable resource for subsequent research to organize and enhance blue OLED technology, fostering continuous progress and innovation in the field.

## 2. Performance of Blue OLEDs

### *2.1. Blue OLED Materials*

The evolution of blue OLED materials has spanned three generations: fluorescent, phosphorescent, and TADF materials [7]. These materials are primarily located in the emissive layer (EML) of OLED devices, situated between the hole transport layer (HTL) and electron transport layer (ETL). This layer is primarily composed of organic molecules or polymers that exhibit high efficiency, long lifetime, and high color purity. Within the light-emitting layer, when an electron, moving to a lower energy state, encounters and fills a hole (a positively charged vacancy left by a missing electron), they recombine to form an exciton. This recombination process involves the electron and hole coming together from their initially separated states. The resulting exciton can exist in two states: the singlet state, where their spins are opposite, and the triplet state, where their spins are aligned [24]. After exciton formation in fluorescent materials, singlet excitons mainly emit light through radiative transition, while triplet excitons cannot emit light due to the energy level difference. Phosphorescent materials enable triplet excitons to transform into singlets through the intersystem crossing (ISC) process, thereby achieving the effect of luminescence. TADF materials combine the advantages of the first two, allowing triplet excitons to undergo thermally activated reverse intersystem crossing (RISC) to transform into singlets and then emit light, achieving efficient and stable exciton utilization [25]. A comparison of the three materials is shown in Figure 2.

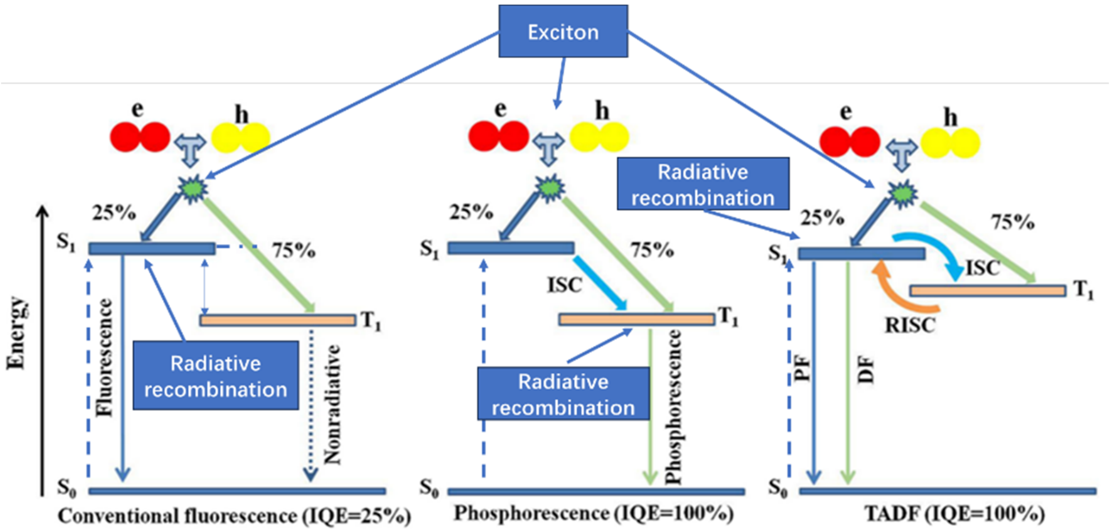

**Figure 2.** Comparative diagram of the process of exciton generation, migration, and decay for conventional fluorescent, phosphorescent, and TADF materials [25]. Reprinted from [25], Copyright (2020), with permission from Elsevier.

Fluorescent OLEDs, the pioneering iteration of this technology, harness organic dyes as their luminous emissive elements. However, they are inherently constrained by the laws of electron spin statistics, enabling only the radiative transition of singlet excitons (accounting for roughly a quarter of all excitons generated) to emit fluorescence. This theoretical limitation inherently caps their luminous efficiency. Blue fluorescent emitters, frequently derived from anthracene derivatives, are renowned for their extensive bandgap, chemically stable structures, robust thermal endurance, and exceptional charge transport capabilities. Nevertheless, the inability to tap into the energy potential of triplet excitons poses a significant hurdle, limiting the EQE of fluorescent OLEDs to approximately 5% [7,26].

To overcome the efficiency limitations posed by fluorescent materials, the second-generation OLEDs introduced heavy-metal complexes as phosphorescent emitters. The enhanced spin–orbit coupling imparted by these heavy-metal atoms, notably iridium and platinum, facilitated efficient radiative transitions from triplet to singlet states, thereby harnessing and exploiting the previously untapped energy of triplet excitons (comprising roughly 75% of total excitons). This groundbreaking approach achieved near 100% IQE in phosphorescent OLEDs, marking a significant leap forward in device performance. In a seminal work in 2001, Adachi et al. [27] attained an EQE of approximately 19.0% and a near-perfect internal phosphorescent efficiency by strategically doping phosphorescent molecules into a wide-bandgap host material. Iridium and platinum complexes have garnered immense attention in the realm of blue phosphorescent OLEDs, owing to their unparalleled performance capabilities. However, the employment of these heavy metals comes at a cost, both financially and environmentally, posing challenges to widespread market adoption and prompting the exploration of alternative, more sustainable solutions [7].

Despite the remarkable achievements of phosphorescent emitters in red and green OLEDs, blue OLEDs continue to grapple with material degradation challenges [28], necessitating the emergence of the third-generation OLED technology: TADF. In a pioneering study in 2012, Zhang's research group at Kyushu University [29] introduced a carbazole/sulfone derivative exhibiting TADF properties, achieving an EQE approaching 10% at low current densities. By facilitating the thermal activation of RISC, TADF materials convert triplet excitons into singlet excitons over extended lifetimes, enabling efficient radiative emission. This innovative mechanism theoretically enables 100% IQE while circumventing the need for heavy metals, addressing cost and environmental concerns. While TADF OLEDs showcase immense potential in harnessing both singlet and triplet excitons efficiently, they are not without their challenges, particularly in mitigating efficiency roll-off at high brightness levels due to exciton-quenching effects. Nevertheless, the advent of TADF technology represents a shift in the OLED landscape, ushering in an era of high-performance, cost-effective, and environmentally benign blue OLED devices, as evidenced by ongoing research and advancements [7,30].

### 2.2. *Performance Metrics*

The luminescence efficiency of blue OLEDs is significantly influenced by the choice of luminescent materials employed. In fluorescent materials, luminescence is predominantly attributed to single-state excitons, whereas phosphorescent and TADF materials can harness both single-state and triplet-state excitons to enhance luminescence efficiency [24]. Currently, a myriad of cutting-edge research efforts is focused on markedly improving the efficiency of converting electron–hole pairs into detectable photons within blue emissive materials, while simultaneously addressing the extension of device lifetime and ensuring good color purity. These advancements in performance are not only crucial for overcoming the prevailing technical constraints of blue OLEDs but are also imperative for driving their progression towards widespread commercialization.

An important parameter in improving the performance of blue OLEDs is EQE. EQE is defined as the ratio of the number of photons emitted from the device to the number of charge carriers (electron–hole pairs) injected into it. For OLED devices, EQE reflects the overall light emission efficiency. When an electric current is applied to the OLED, electrons and holes are injected into the light-emitting layer, where they recombine to form excitons. These excitons then decay radiatively, emitting photons. The EQE can be expressed using the following formula [31] (p. 5):

$$\mathrm{EQE} = \eta_{\mathrm{rec}}\eta_{\mathrm{spin}}\eta_{\mathrm{rad}}\eta_{\mathrm{out}} = \mathrm{IQE}\cdot\eta_{\mathrm{out}}, \tag{1}$$

where the charge recombination efficiency ($\eta_{rec}$) measures the proportion of injected electrons and holes that successfully recombine to form excitons. Ideally, all injected charges are expected to recombine into excitons, resulting in an ideal value of $\eta_{rec}$ equal to 1. Spin efficiency ($\eta_{spin}$) reflects the proportion of the formed excitons that are capable of emitting light. For fluorescent OLEDs, where only singlet excitons can emit light, this ratio is typically around 25%. In contrast, for phosphorescent OLEDs, $\eta_{spin}$ can approach 100%, as triplet excitons can also emit light. TADF materials can reverse the spin of triplet excitons to singlet excitons through thermal activation, enabling fluorescence emission; thus, their $\eta_{spin}$ also approaches 100%. Radiative efficiency ($\eta_{rad}$) indicates the probability that the generated excitons decay via radiative recombination (i.e., emission of photons) rather than non-radiative decay processes (such as thermal dissipation). This factor measures the photoluminescence quantum efficiency of the emitting material, with $\eta_{rad}$ ideally being 1. The product of $\eta_{rec}$, $\eta_{spin}$, and $\eta_{rad}$ gives the IQE, which reflects the overall efficiency of exciton formation from charge injection to radiative recombination within the device. Light outcoupling efficiency ($\eta_{out}$) represents the proportion of emitted light that ultimately exits the OLED and is observable. Due to absorption or reflection losses in the material, $\eta_{out}$ is typically around 20%. The product of IQE and $\eta_{out}$ constitutes EQE. EQE reflects the device's ability to convert injected electron–hole pairs into photons that can escape the device and be detected externally. To enhance the overall performance of light-emitting devices, it is essential to optimize these individual efficiencies. This involves improving device structure, material selection, and fabrication processes to enhance charge injection efficiency, minimize non-radiative losses, and improve light coupling output, thereby ultimately achieving higher EQE [32,33].

Another crucial metric is the operational lifetime of blue OLED, typically assessed by collecting data on brightness decay under constant current drive. Lifetime indicators such as $LT_{50}$ and $LT_{95}$ measure the time it takes for brightness to decrease to 50% and 95% of the initial luminance, respectively, providing standardized evaluations. However, for high-resolution OLED displays, this conventional measurement appears basic. The performance of each subpixel can significantly impact the overall display quality, necessitating more advanced measurement methods such as the Stretched Exponential Decay model to evaluate and enhance individual subpixel performance [34,35].

In addition, for pure-blue OLEDs, the narrowness of the FWHM of the emission spectrum as well as power efficiency (PE) and current efficiency (CE) significantly impact spectral quality, color reproduction, and energy utilization. High color purity indicates that the OLED can more accurately reproduce the target color, which is often achieved through technologies such as optical microcavities or optical filters. However, when the emission spectrum of the OLED is very broad, these techniques, while improving color purity, may result in excessive filtration of spectral components, leading to reduced brightness and thus diminished overall luminous efficiency. Optimizing the FWHM of the OLED can achieve a narrower emission spectrum, reducing the emission of non-target wavelengths and concentrating more light energy at the desired wavelength. This improvement not only significantly enhances color purity but also reduces spectral energy waste in certain applications, thereby indirectly improving overall light conversion efficiency. Furthermore, advanced materials and technologies, such as TADF materials and hyperfluorescence techniques, enhance both exciton utilization and minimize spectral energy loss, leading to increased color purity and directly improving OLED luminous efficiency. These factors underscore the importance of optimizing FWHM and employing advanced technologies to enhance both color purity and light conversion efficiency. Consequently, addressing color purity through molecular design or novel OLED fabrication techniques is crucial [16]. PE measures the luminous power output relative to the input electrical power, indicating the efficiency with which the device converts electrical energy into light. It is typically expressed as the ratio of output light power to input electrical power, reflecting the device's light conversion capability. CE represents the light flux produced per unit current, emphasizing the efficient conversion of electrical current into visible light. It is usually quantified in terms of the luminous flux per ampere of current, reflecting the efficient utilization of current while maximizing brightness. By improving the CE and PE of blue OLEDs, higher light output can be achieved with the same input electrical power, thereby reducing power consumption and promoting energy savings. Moreover, high CE and PE help maintain or enhance brightness while reducing energy losses, ensuring a balance between brightness and efficiency.

## 3. High-Efficiency Blue OLED Materials

In recent years, with the rapid development of display and lighting technologies, the enhancement of blue OLED performance, as the fundamental element of next-generation display technology, has garnered significant attention from both the scientific research community and the industry. Particularly, in the realm of materials research, scientists have consistently overcome the limitations of the optoelectronic performance of blue OLEDs through inventive molecular designs and strategies. This section will examine a range of significant advancements achieved in recent years in the areas of fluorescent, phosphorescent, and TADF materials for blue OLEDs.

### *3.1. High-Efficiency Fluorescent Materials*

In recent studies, some fluorescent materials have been used to optimize the optoelectronic performance of blue OLEDs by designing specific molecular structures and chemical modifications. In 2022, Xiao et al. [36] introduced two deep-blue OLED fluorescent materials, 2-(4′-(9,9-dimethylacridin-10(9H)-yl)-[1,1′-biphenyl]-4-yl)-1phenyl-1H-phenanthro[9,10-d]imidazole (DP) and 10-(4′-(1-phenyl-1H-phenanthro[9,10-d]imidazol-2-yl)-[1,1′-biphenyl]-4-yl)-10H-spiro[acridine-9,9′-fluorene] (SP), both featuring phenanthroimidazole (PPI) derivatives as acceptors (Figure 3a). These materials exhibit efficient hybrid local and charge-transfer (HLCT) properties, accompanied by high photoluminescence quantum yield (PLQY) and excellent color purity. This study showed that while DP achieved a maximum EQE of 6.4%, the nondoped OLED based on SP reached an EQE maximum ($\mathrm{EQE_{max)}}$ of 11.3%, representing a commendable achievement among non-delayed, nondoped deep-blue fluorescent OLEDs (Figure 3b). Additionally, at a wavelength of 436 nm, DP and SP achieved PLQYs of 40% and 62%, respectively. This accomplishment not only showcases two high-performance deep-blue HLCT emitters but also demonstrates the achievement of a high horizontal dipole orientation through optimized molecular structures, significantly enhancing OLED's luminous efficiency and color purity. This work provides novel materials and design insights for the advancement of blue OLED technology. In 2024, Chen and co-workers [37] successfully developed two novel blue fluorescent materials, SAFPI–3 and SAFPI–2, whose electronic structure characteristics within the framework of molecular orbital theory are illustrated in Figure 3c. These materials, based on phenanthroimidazole derivatives, address the scarcity of highly efficient, short-wavelength blue fluorescent materials in the market. By manipulating the molecular structures, SAFPI–3 achieved a remarkable photoluminescence quantum yield of up to 96% in neat films, significantly outperforming SAFPI–2, which had a yield of 41%. OLED devices based on SAFPI–2 and SAFPI–3 attained maximum EQE of 3.83% and 4.99%, respectively (Figure 3d). As host materials for OLEDs, both SAFPI–3 and SAFPI–2 exhibited exceptional performance in both light-blue and yellow OLEDs, particularly with slight efficiency roll-off at high brightness levels. Consequently, SAFPI–3 and SAFPI–2 also hold potential as matrix materials for hosting other emitters.

Fluorescent zinc (II) complexes have also garnered attention for their excellent luminescent properties [38]. In 2021, Liu and his colleagues [39] synthesized a novel zinc complex, Zn(PhCzKt)$_2$, where PhCzKt represents dehydrogenation 1-(4-(tert-butyl)phenyl)-3-(9-ethyl-9H-carbazol-3-yl)propane-1,3-dione. This zinc complex employs β-diketone molecules as chelating ligands and is adorned with carbazole and tert-butyl phenyl substituents (Figure 3e). Utilizing triethylamine as a catalyst, this complex exhibited remarkable thermal stability and electrochemical properties, which were comprehensively characterized through spectroscopic and other analytical methods. Density functional theory (DFT) calculations unraveled its luminescent mechanism, involving an electron transition from the lowest unoccupied molecular orbital (LUMO) primarily residing on the phenyl group to the highest occupied molecular orbital (HOMO) predominantly located on the carbazole unit. Electroluminescent devices fabricated from Zn(PhCzKt)$_2$ displayed a distinct deep-blue emission with CIE color coordinates of (0.1558, 0.0901). Eventually, these devices achieved a maximum EQE of 1.54%, suggesting that further structural optimization holds promise for enhancing device performance in the future. In 2022, Solanki and colleagues [40] successfully synthesized two blue-emissive Zn(II) complexes, Zn–1 and Zn–2, incorporating pyrazolone-based azomethine ligands (Figure 3f). The solid-state structures of these complexes exhibit enhanced rigidity compared to their solution counterparts, a characteristic that facilitates the suppression of non-radiative transitions, thereby elevating their photoluminescence quantum yields. The naphthalene core in Zn–1 displays a more rigid arrangement in comparison to the butoxyphenyl core in Zn–2, resulting in Zn–1 demonstrating a higher photoluminescence quantum yield and superior device performance. Eventually, OLED devices utilizing Zn–1 achieved a maximum EQE of 3.2%, concurrently emitting deep-blue light with a CIE$_y$ coordinate of 0.09, fulfilling the requirements for high color saturation in display technologies.

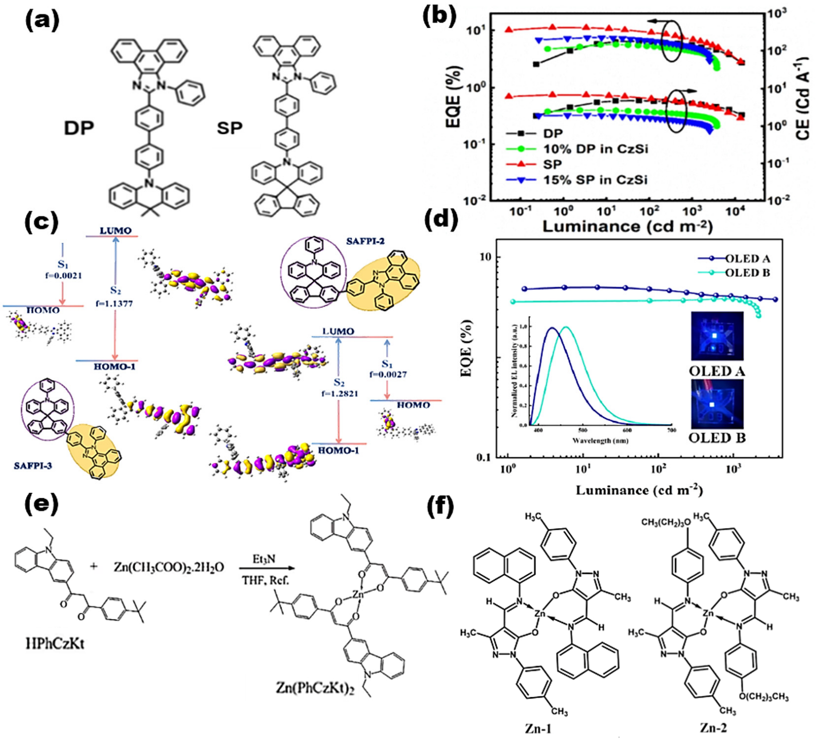

**Figure 3.** (**a**) The chemical structure of DP and SP. (**b**) EQE–luminance –CE characteristic curves of DP and SP. The circles and arrows indicate that the upper curve is the EQE–luminance curve, while the lower curve is the CE–luminance curve. [36]. (**c**) The chemical structure of SAFPI–2 and SAFPI–3. (**d**) Luminance–EQE characteristics (inset: EL spectra) [37]. (**e**) Synthetic route of Zn(PhCzKt)$_2$ [39]. (**f**) The chemical structure of bidentate zinc complexes Zn–1 and Zn–2 [40]. (**a**,**b**): Reprinted from [36], Copyright (2022), with permission from Elsevier. (**c**,**d**): Reprinted from [37], Copyright (2024), with permission from Elsevier. (**e**): Reprinted from [39], Copyright (2022), with permission from Elsevier. (**f**): Reprinted from [40], Copyright (2022), with permission from Elsevier.

Recent studies have focused on the innovative mechanisms underlying blue and deep-blue fluorescent OLED materials, achieving significant advancements through the implementation of the hot exciton pathway, which has led to remarkable improvements in device efficiency and stability, offering valuable insights for the future development of OLED technology. In 2019, Xu et al. [17] introduced a novel blue fluorescent emitter, 2-(4-(10-(3-(9H-carbazol-9-yl)phenyl)anthracen-9-yl)phenyl)-1-phenyl-1H-phenanthro[9,10-d]imidazole (PAC), composed of phenanthroimidazole substituted with phenylcarbazole and anthracene (Figure 4a). The key innovation lies in the utilization of a new mechanism: the reverse intersystem crossing (RISC) from the high-energy triplet state to the singlet state, known as the "hot exciton" path. The newly designed blue fluorescent emitter material, PAC, combined with a specific energy level structure, facilitates the rapid RISC process from a triplet state to a singlet state, enabling efficient blue fluorescent emission. As depicted in Figure 4b, the PAC-based undoped device achieves a maximum EQE of 10.48% with a small efficiency roll-off. Additionally, this device exhibits excellent spectral stability, ensuring consistent light output, as well as superior color purity with CIE coordinates of (0.15, 0.13). This research has overcome the limitation of traditional fluorescent OLEDs, where efficiency is typically restricted by the radiative decay of singlet excitons, capping the IQE at 25%. By utilizing the "hot exciton" pathway, the efficiency of blue fluorescent OLEDs has been significantly enhanced, approaching the level of phosphorescent OLEDs. This provides valuable insights for the development of efficient and stable blue and deep-blue fluorescent OLEDs. In 2022, Yang et al. [41] presented an efficient blue OLED sensitized by hot exciton fluorescent nanoaggregates (HENAs), with the device structure shown in Figure 4c. By utilizing the high-mobility crystalline material 2-(4-(9H-carbazol-9-yl)phenyl)-1(3,5-difluorophenyl)-1H-phenanthro[9,10-d]imidazole (2FPPICz) and the highly luminescent PAC nanoaggregates operating at low voltages, they significantly enhanced EQE to 9.14%. Additionally, they lowered the driving voltage with a turn-on voltage of just 2.5 V and an operating voltage of only 3.3 V at 1000 cd/m$^2$, reduced energy losses with a Joule heating loss ratio of 7.8% at 1000 cd/m$^2$, and improved thermal stability and color purity. This research effectively addresses the issue of low photon emission efficiency in traditional amorphous thin-film OLEDs under low driving voltages, significantly enhancing the performance and practicality of OLED devices. In 2023, Du et al. [42] designed and synthesized two efficient deep-blue emitters, PITPh and PPITPh (Figure 4d). PITPh showed a PLQY of 32.83% with an emission peak at 432 nm in vacuum-deposited thin films, while PPITPh, due to the incorporation of a benzene bridge, exhibited enhanced oscillator strength (1.2705) and a high PLQY of 77.37% with an emission peak at 441 nm in vacuum-deposited thin films. They achieved efficient utilization of triplet excitons through the RISC process under the hot exciton mechanism in a nondoped device architecture, thereby further enhancing device performance. As shown in Figure 4e, the nondoped OLED utilizing PPITPh as the emissive layer demonstrated exceptional EQE$_{max}$ (11.83%) alongside stable deep-blue emission, maintaining high efficiency even at high brightness levels, exemplifying the effective exploitation of triplet excitons via the hot exciton pathway. Additionally, PPITPh served as an outstanding host material in doped phosphorescent organic light-emitting diodes (PhOLEDs), achieving high EQE$_{max}$, underscoring its versatility and application potential. This study provides significant theoretical support for the development of novel high-efficiency OLED materials. In the same year, Park et al. [33] conducted an in-depth study and analysis on the significant advantages of the hot exciton mechanism in improving OLED performance and stability. This mechanism can effectively enhance the utilization rate of singlet excitons, improve device stability and lifetime, and boost luminescent efficiency through flexible molecular design. However, this mechanism currently faces several challenges, such as inadequate theoretical explanations, high computational costs, the complexity of experimental verification, and difficulties in material design and device integration. Therefore, despite the vast potential of the hot exciton mechanism in enhancing OLED performance and stability, overcoming these challenges is necessary for its widespread application.

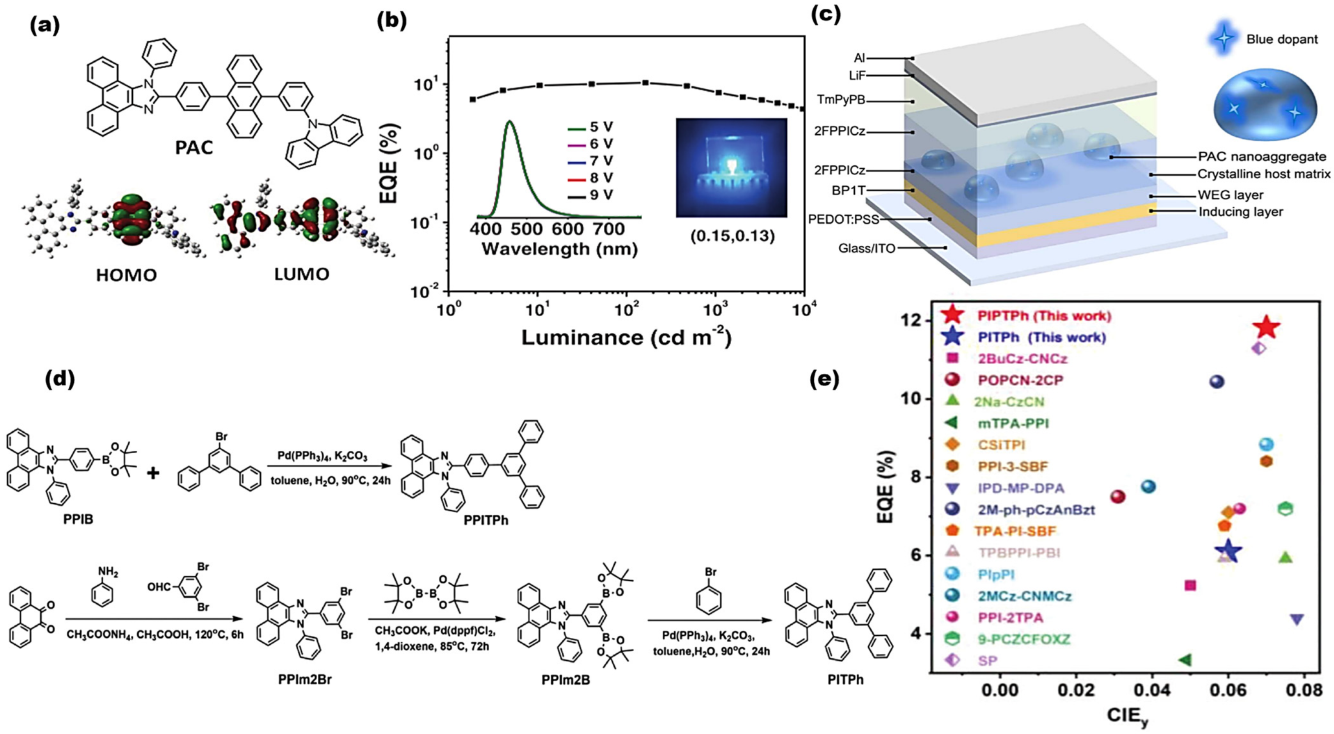

**Figure 4.** (**a**) Molecular structure and the HOMO and LUMO distributions of PAC. (**b**) EQE versus luminance for the device. The photo inserted shows the electroluminescent spectra at different voltages, an emission picture of the device, and its CIE value [17]. (**c**) Schematic diagram of device structure [41]. (**d**) Synthesis route of PPITPh and PITPh. (**e**) Relationship between EQE$_{max}$ and CIE$_y$ [42]. (**a**,**b**): Reprinted from [17], Copyright (2019), with permission from WILEY. (**d**,**e**): Reprinted from [42], Copyright (2023), with permission from WILEY.

### *3.2. High-Efficiency Phosphorescent Materials*

In the realm of phosphorescent material design, Feng et al. [43] in 2020 devised and synthesized a series of heavy-metal-free, carbonyl-free, purely organic emitters (TCz-F, TCz-H, TCz-OH) based on commercially available or laboratory-synthesized carbazoles and benzenes. The chemical formulas and physical properties of these emitters are illustrated in Figure 5a. By harnessing the push–pull electron effect, they modulated the molecular emission of these organic emitters, transitioning from fluorescence to phosphorescence. Notably, they discovered that altering the substituent groups could significantly impact the photophysical properties of the molecules, leading to the development of highly efficient blue and white organic light-emitting devices. This research provides a novel theoretical foundation for the design and regulation of organic light-emitting materials. In 2021, Ye et al. [44] took an alternative approach by confining isolated chromophores within a rigid crystalline matrix to achieve efficient blue phosphorescence emission. They selected pyromellitic acid (PMA), featuring four carboxylic acid groups, as the model chromophore and transformed it into tetrasodium pyromellitate (TSP) through sodiation, subsequently constructing an ionic crystal. Leveraging the rigid molecular network formed by ionic bonding, they effectively suppressed non-radiative transitions, thereby significantly enhancing phosphorescence efficiency. The TSP crystal exhibited a maximum phosphorescence lifetime of 168.39 ms at room temperature, with a maximum phosphorescence quantum yield reaching 96.5% (Figure 5b). This methodology offers a novel avenue for the development of long-lived, high-efficiency blue phosphorescent materials. In 2022, Kong et al. [45] explored the application of pure hydrocarbon materials as efficient phosphorescent OLED hosts, leveraging the C1 position of the 9,9′-spirobifluorene (SBF) scaffold for molecular design. They synthesized three distinct pure hydrocarbon host materials: 1-p-SBF, 1-mbp-SBF, and 1-mtp-SBF. The synthetic routes for these materials are illustrated in Figure 5c. These heteroatom-free pure hydrocarbon materials demonstrated remarkable performance in blue PhOLEDs. As shown in Figure 5d, a device utilizing 1-mtp-SBF as the host achieved an EQE of 25.6%, marking the first time that a PhOLED employing a PHC host and FIrpic blue emitter surpassed the 25% threshold.

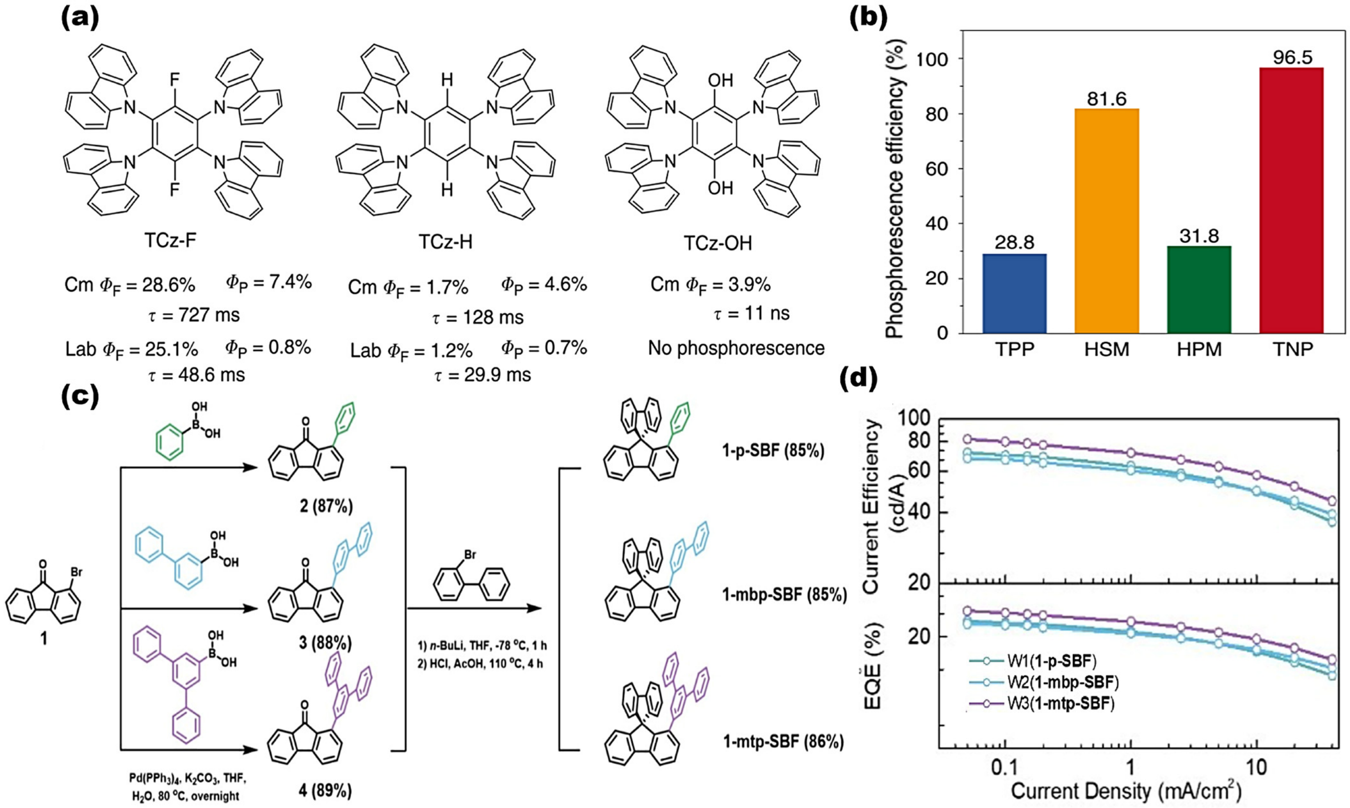

**Figure 5.** (**a**) Molecular structures and photophysical properties [43]. (**b**) Measured phosphorescence efficiencies of the phosphors [44]. (**c**) Synthesis of PHC hosts. (**d**) CE and EQE of PhOLEDs using 1pSBF, 1mbpSBF, and 1mtpSBF as hosts, respectively [45]. (**b**): Reprinted from [44], reproduced with permission from SNCSC. (**c**,**d**): Reprinted from [45], Copyright (2022), with permission from WILEY.

In 2022, Zhou et al. [46] devised an innovative approach by blending a phosphorescent material, bis[2-(4,6-difluorophenyl)pyridinato-C2,N]iridium(III) (FIrpic), with a TADF material, 10,10′-(4,4′-sulfonylbis(4,1-phenylene))bis(9,9-dimethyl-9,10-dihydroacridine) (DMAC-DPS), and doping them in a certain ratio into a host material, 1,3-bis(carbazol-9-yl)benzene (mCP), to construct a hybrid emission system, specifically a TADF-phosphorescent mixed-light-emitting system. As illustrated in Figure 6a, the introduction of phosphorescent materials significantly enhances exciton utilization and effectively reduces excess carriers. As a result, compared to undoped devices, doped devices exhibit higher current efficiency under the same voltage. At doping concentrations of 0.2 wt%, 1 wt%, and 3 wt%, as the current density increases, if the exciton recombination rate cannot keep pace with exciton generation, excess excitons will decay through non-radiative pathways, leading to a decrease in luminous efficiency. Consequently, devices with different doping concentrations will achieve maximum current efficiency at different current densities, forming a peak in the efficiency–current density curve. At low concentrations, energy transfer efficiency gradually increases with rising doping concentration. However, at excessively high concentrations, concentration quenching may occur, resulting in a decrease in efficiency. As shown in the figure, at a doping concentration of 1 wt%, exciton generation and recombination reach an optimal balance, achieving a maximum current efficiency of 21.1 cd/A at the lowest current density. This methodology not only reduces the usage of expensive phosphorescent materials but also maintains the high-performance characteristics of the device. In 2024, Jung et al. [47] employed theoretical simulations, encompassing molecular dynamics and quantum chemical simulations, to design complexes with the aim of mitigating the metal-to-metal-to-ligand charge-transfer (MMLCT) effect and enhancing device performance. Through strategic modifications to the t-butyl positions in tetradentate Pt(II) complexes, two novel Pt(II) complexes, PtON-tb-DTB and PtON-tb-TTB, were synthesized (Figure 6b). These complexes effectively suppressed the formation of MMLCT, leading to a significant extension of the lifetime of blue phosphorescent OLEDs. When employed as blue phosphorescent dopants in OLED devices, the $LT_{95}$ values at an initial luminance of 1200 cd $m^{-2}$ were recorded as 169.3 h and 31 h, respectively, for PtON-tb-DTB and PtON-tb-TTB. Furthermore, as shown in Figure 6c, these devices achieved a maximum EQE of up to 26.3% and 20.9%, respectively.

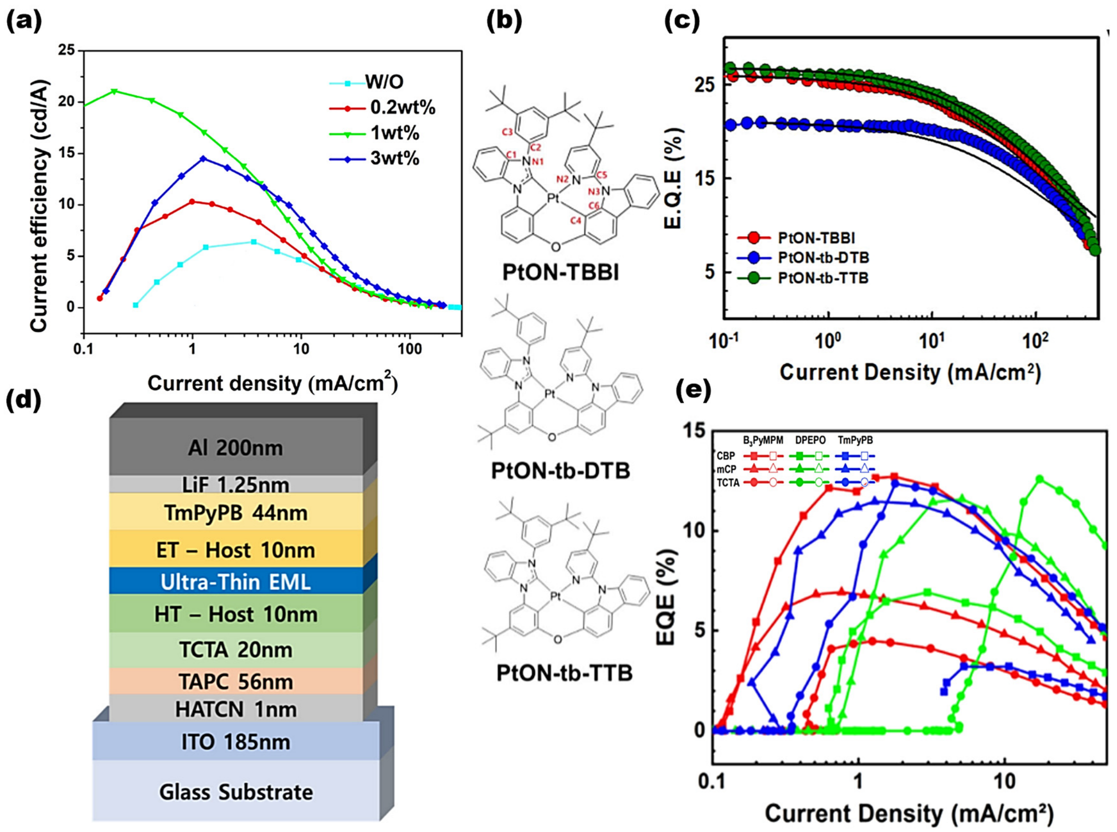

**Figure 6.** (**a**) CE versus current density characteristics of OLEDs with different doping concentrations of FIrpic in EML [46]. (**b**) Molecular structures of PtONTBBI, PtONtbDTB, and PtONtbTTB. (**c**) EQE–current density of PtONTBBI, PtONtbDTB, and PtONtbTTB [47]. (**d**) Fabricated OLED device structure. (**e**) Current density–EQE characteries [30]. (**a**): Reprinted from [46], Copyright (2022), with permission from Elsevier.

In the research on OLED degradation mechanisms, Trindade et al. [48] in 2023 employed nanoscale chemical depth profiling techniques to conduct chemical depth analyses on blue phosphorescent and TADF OLED devices with varying degradation levels. They directly identified the interfacial degradation products and their distributions within blue OLEDs. Their findings revealed that the primary degradation pathway involves oxygen loss at the interface between the EML and the ETL. By altering the host material, they mitigated degradation at the EML/ETL interface, demonstrating approximately an order of magnitude improvement in device lifetime. This work provides crucial insights for future material selection and device architecture design.

In the context of structural optimization for blue OLEDs, Jang and co-workers [30] in 2023 employed a prototypical blue phosphorescent material, FIrpic, and investigated the impact of varying transport layer material combinations on device performance. Their findings revealed that an undoped ultra-thin emissive-layer (U-EML) architecture, as depicted in Figure 6d, coupled with strategic material selection and thickness optimization, could significantly enhance the efficiency of blue OLEDs. As shown in Figure 6e, FIrpic consistently maintained high efficiency when paired with diverse charge transport layers (such as CBP, mCP, and TCTA) and electron transport layers (including $B_3$PyMPM, DPEPO, and TmPyPB). This study showed that FIrpic achieved a maximum EQE of 12.7%, indicating its strong suitability for high-efficiency ultra-thin EML blue OLEDs.

Combining fluorescent emitters with sensitizing materials (or sensitizers) in OLEDs, hyper-OLED technology enables high efficiency and long operation times. A number of phosphorescent sensitizing materials have been recently designed. In 2021, Lee et al. [49] conducted a study on PSF-OLED structure, incorporating a phosphorescent sensitizer Ir(cb)$_3$ and a fluorescent dopant t-DABNA. They initially optimized the OLED performance by varying the doping concentration of t-DABNA, identifying 1 wt.% as the optimal condition. This optimized doping level was then employed in a PSF-OLED containing 10 wt.% of the Ir(cb)$_3$ sensitizer. This study revealed that the phosphorescent sensitizer not only facilitated energy transfer but also significantly improved the charge balance and operating voltage of the device (Figure 7a). Consequently, they successfully achieved a deep-blue PSF-OLED with high efficiency (EQE = 21.6%) and low driving voltage by optimizing the doping concentration of the phosphorescent sensitizer. This work presents novel insights and methodologies for advancing the development of blue OLEDs. In the same year, Nam et al. [50] made remarkable advancements in the field of OLED technology by innovatively introducing Pt(II) complex (PtON7-dtb) as an efficient phosphorescent sensitizer. This was integrated with two advanced emitters, namely, a hydrocarbon-based fluorophore (TBPDP) and a multiple resonance fluorophore (ν-DABNA), within the EML of the device. Their chemical molecular formulas are shown in Figure 7b. This design ingeniously achieved a highly efficient energy transfer mechanism from the triplet excited state of the phosphorescent sensitizer to the singlet excited state of the emitters, significantly enhancing the luminescent performance of the OLEDs. Experimental results demonstrated that OLEDs based on TBPDP and ν-DABNA emitters achieved maximum EQE of 16.9% and 32.2%, respectively. As shown in Figure 7c,d, the chromaticity coordinates of these OLEDs fell within the blue region, confirming their stable emission of deep-blue light. Eventually, under a brightness of 1000 cd m$^{-2}$, the EQE of ν-DABNA-based OLEDs significantly surpassed that of TBPDP-based OLEDs, showcasing its superior luminous efficacy. Additionally, in terms of device lifetime, the LT$_{50}$ (half-lifetime) of TBPDP-based OLEDs reached 192.2 h at 1000 cd m$^{-2}$ brightness, while ν-DABNA-based OLEDs exhibited a remarkable 19-fold extension in lifetime, with an LT$_{50}$ as high as 253.8 h. These data not only underscore the stability advantage of TBPDP material but also further validate the substantial improvements in maximum current efficiency and half-lifetime of hyperfluorescent OLEDs compared to conventional phosphorescent OLEDs. In 2023, Wu et al. [51] synthesized two novel [3+2+1] iridium complexes, B–4–TMS and B–5–TMS, by incorporating bulky trimethylsilyl (TMS) groups. These complexes were employed as blue phosphorescent sensitizers in OLEDs, with the synthesis process illustrated in Figure 7e. These complexes not only enhanced the triplet-exciton harvesting efficiency but also significantly improved the color purity and EQE of blue OLEDs. Figure 7f–h present some key performance parameters of devices C-F, where devices C and D utilize CzSi as the host material, with B—-TMS (12.5%) and B–5–TMS (12.5%), respectively, acting as sensitizers for the terminal emitter v–DABNA (1%). In contrast, devices E and F employ SiCzCz:SiTrzCz2 as the host material, with B–4–TMS (12.5%) and B–5–TMS (12.5%), respectively, serving as sensitizers for the terminal emitter v–DABNA (1%). Devices E and F achieved maximum EQEs of 33.43% and 33.42%, respectively, accompanied by impressive lifetimes and color purities. This work by Wu et al. demonstrates the potential of molecular design in enhancing the performance of OLEDs.

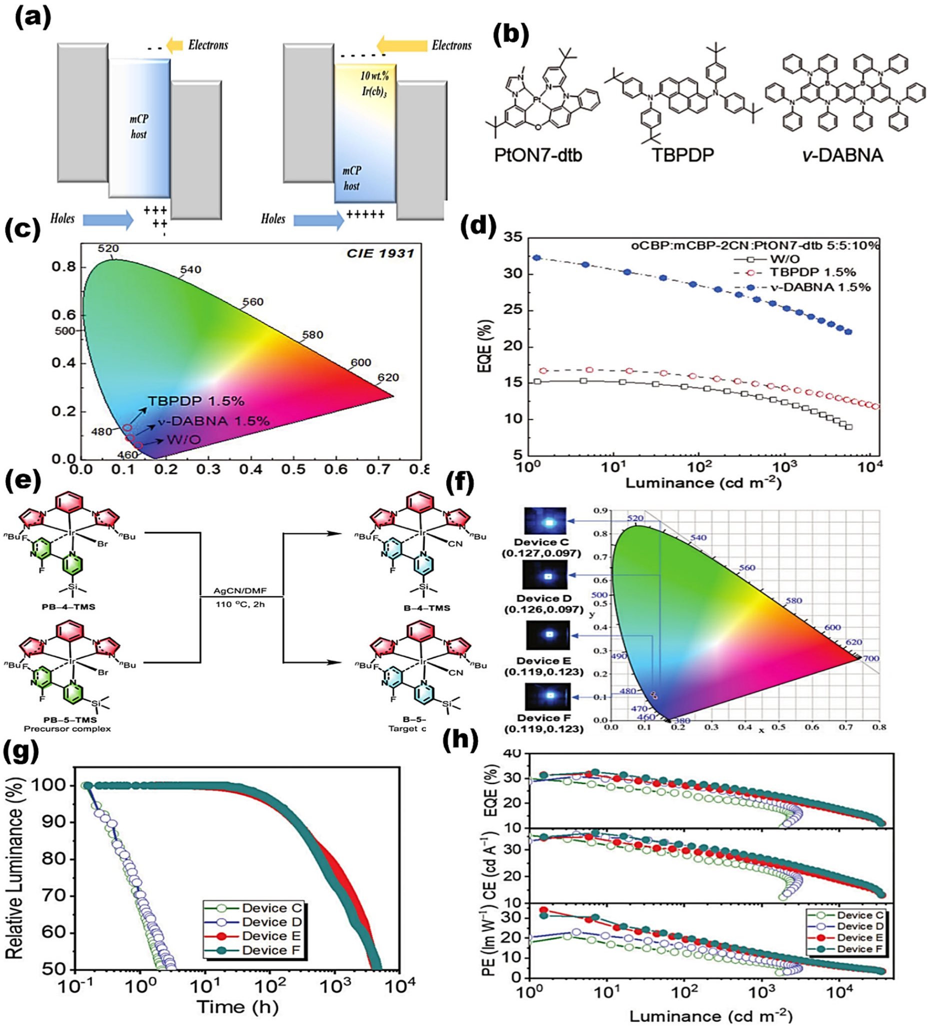

**Figure 7.** (**a**) Operational mechanisms of the device with 1 wt.% of tDABNA doped in mCP as the EML and the device that incorporates both the Ir(cb)$_3$ sensitizer and the optimized doping concentration of tDABNA (1 wt.%) [49]. (**b**) Chemical structures of the PtON7dtb Ph sensitizer and the TBPDP and *ν*DABNA emitters. (**c**) CIE chromaticity coordinates. (**d**) Normalized electroluminescence spectra of bottom emission for the control device (PtON7dtb 10%) and 1.5% TBPDP and *ν*DABNA hyperOLED devices at a luminance of 1000 cd m$^{-2}$ [50]. (**e**) Synthesis of iridium complexes B–4–TMS and B–5–TMS. (**f**) CIE coordinates and images of the devices. (**g**) Device lifetime curves at 100 cd m$^{-2}$. (**h**) EQE, CE, and PE versus luminance [51].

### *3.3. High-Efficiency TADF Materials*

Recent research in TADF materials for high-efficiency blue organic light-emitting diodes has been very active, significantly advancing OLED technology. Significant progress has been made in enhancing the efficiency of blue OLEDs by designing innovative TADF molecular structures. In 2020, Kim et al. [52] developed an efficient deep-blue TADF emitter, TMCz-BO, featuring 1,3,6,8-tetramethyl-9H-carbazole (TMCz) as the donor and 5,9-dioxa-13-boranaphtho[3,2,1-de] anthracene (BO) as the acceptor (as shown in Figure 8a). By incorporating a rigid acceptor structure and specific functional groups, this molecule minimizes molecular vibrations, thereby achieving a narrow emission spectrum. Leveraging the nanosecond-scale delayed fluorescence property of TMCz-BO, the accumulation of triplet excitons is effectively suppressed, enabling the conversion of triplet excitons into singlet excitons and subsequent radiative emission, achieving an IQE approaching 100%. As shown in Figure 8b, compared to TMCz-3P (consisting of 3,11-diphenyl-5,9-dioxa-13b-boranaphtho[3,2,1-de]anthracene(3P) as the acceptor), TMCz-BO exhibits a higher maximum EQE, reaching up to 20.7% at low current densities while significantly mitigating the issue of efficiency roll-off. This study provides a methodology for the development of novel TADF materials. In 2022, Naveen et al. [53] designed and synthesized three deep-blue TADF emitters, namely, m-ν-DABNA, 4F-ν-DABNA, and 4F-m-ν-DABNA, characterized by high quantum efficiency and narrowband emission properties. By strategically incorporating methyl and fluorine atoms into the diboron-based ν-DABNA core structure, these emitters underwent modulation of their electronic structures, resulting in a blueshift and narrowing of the emission spectra, thereby enhancing color purity. Their synthetic routes and chemical formulas are depicted in Figure 8d. The three emitters, m-ν-DABNA, 4F-ν-DABNA, and 4F-m-ν-DABNA, all achieved a PLQY of around 90% at wavelengths of 455 nm, 447 nm, and 446 nm, respectively, indicating their remarkable ability to efficiently convert nearly all absorbed photons into emitted light, achieving exceptional efficiency in light energy conversion. Their small singlet–triplet energy gaps ($\Delta E_{ST}$) values (not exceeding 0.07 eV) facilitate rapid and efficient transitions of electrons between energy states, optimizing the emission process. The fast reverse intersystem crossing rates (kRISC) enhance triplet state utilization. Their maximum EQE reached 36.2%, 35.8%, and 33.7%, respectively (Figure 8c), demonstrating outstanding device efficiencies that ensure efficient energy transfer and bright emission. Furthermore, the design methodologies outlined in this research serve as a solid foundation for advancing the development of multiple-resonance TADF (MR-TADF) emitters exhibiting hypsochromic shifts, thereby paving new paths for exploration and innovation.

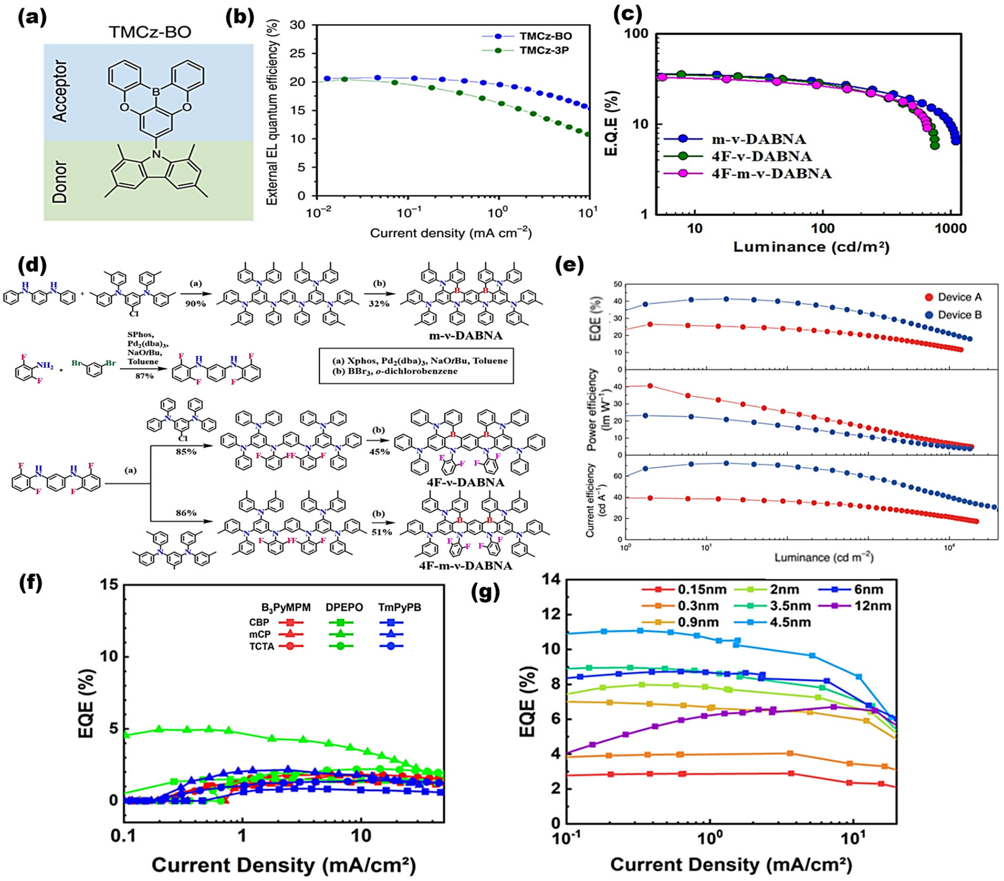

**Figure 8.** (**a**) Molecular structures of TMCz-BO. (**b**) External EL quantum efficiency versus luminance plots of TMCz-BO- and TMCz-3P-based OLEDs [52]. (**c**) EQE versus luminance plot. (**d**) Synthetic route for all the designed MR emitters [53]. (**e**) EQE, CE, and PE versus luminance of devices A and B [19]. (**f**) Current density–EQE characteristics. (**g**) Current density–EQE characteristics [30]. (**c**,**d**): Reprinted from [53], Copyright (2022), with permission from Elsevier. (**e**): Reprinted from [19], reproduced with permission from SNCSC.

Optimization of the device structure is also an important way of improving the efficiency of blue OLEDs. In 2021, Chan et al. [19] designed a TADF sensitizer, TPh2Cz2DPhCzBN (HDT-1), to sensitize the pure-blue emitter ν-DABNA. A dual-unit-stacked tandem OLED structure was employed, leveraging the high RISC rate of HDT-1 to rapidly convert triplet excitons into singlet excitons, thereby reducing the triplet-exciton density and enhancing device lifetime. Concurrently, efficient energy transfer was achieved by co-depositing the TADF assistant dopant with the pure-blue fluorescent emitter, improving emission color purity. As illustrated in Figure 8e, Device A and Device B utilized the same emissive-layer material combination (with mCBP as the host, doped with 0.5% of ν-DABNA fluorescent material and 20% of HDT-1 TADF material). However, Device B featured a dual-unit-stacked tandem architecture, enabling it to achieve an EQE of 32% at a luminance of 1000 cd $m^{-2}$ and a maximum EQE of 41%. Additionally, this OLED maintained a highly pure-blue light output (CIE coordinates of (0.13, 0.16)), narrow emission spectrum (FWHM of 19 nm), and long initial luminance retention ($LT_{95}$ of 18 h). This innovative pure-blue OLED technology addresses the challenges of color purity, efficiency, and lifetime. It is anticipated that, through optimization of the manufacturing process, the lifetime will further improve, rivaling that of commercial fluorescent blue OLEDs. In 2023, Jang et al. [30] investigated the application of a U-EML structure in blue OLEDs, utilizing undoped DMAC-DPS material. They initially examined the performance of DMAC-DPS when combined with various charge transport layers (such as CBP, mCP, and TCTA) and electron transport layers (including $B_3$PyMPM, DPEPO, and TmPyPB), observing that the EQE of each DMAC-DPS combination was not only low but also exhibited significant disparities (Figure 8f). Subsequently, they aimed to improve the performance by adjusting the thickness of the DMAC-DPS U-EML. As shown in Figure 8g, a maximum EQE of 11.1% was achieved at a thickness of 4.5 nm, demonstrating the ability to maintain high efficiency even in thicker emitting layers. This study underscores that optimizing the thickness of the U-EML and selecting appropriate transport layer materials can substantially enhance the EQE of blue OLEDs.

Fine control of charge-transfer, excited-state properties, and energy gap modulation within the TADF molecule enables highly efficient and stable blue OLEDs. In 2020, Zhang et al. [54] investigated the impact of excited-state properties on the performance of four quaternary bipolar host materials (9ArFDBFxPO) featuring an insulating donor–acceptor (D-A) architecture in OLED devices. The synthesis and chemical molecular structures of 9ArFDBFxPO are depicted in Figure 9a. By modulating the intramolecular interactions between donor and acceptor moieties, the exciton binding energy ($E_b$) of the hosts was reduced, fostering Dexter energy transfer towards blue dopants, particularly blue TADF dyes, thereby enhancing the efficiency of OLEDs. Eventually, blue PH and TADF OLED devices based on 9-(4-(9-(4-(4,6-bis(diphenylphosphoryl)dibenzo[b,d]furan-2-yl)phenyl)-9H-fluoren-9-yl)phenyl)-9H-carbazole (9CzFDBFDPO) achieved an EQE exceeding 20% at 100 cd $m^{-2}$ with minimal efficiency roll-off at high brightness. As shown in Figure 9b, devices incorporating 9CzFDBFDPO as the host with different dopants, FIrpic and DMAC-DPS, attained maximum EQE of 23.3% and 20.2%, respectively. This study underscores the potential of bipolar hosts for commercial applications. In the same year, Zheng et al. [55] introduced a molecule named T-CNDF-T-*t*Cz, featuring a multi-donor/-acceptor structure with three donor (D) and three acceptor (A) units. This architecture, leveraging the through-space charge-transfer (TSCT) effect, enables the material to exhibit a small $\Delta E_{ST}$ and a high transition dipole moment. Meanwhile, the through-bond charge-transfer (TBCT) effect, by promoting degenerate molecular orbitals, facilitates multi-channel RISC, enhancing the utilization of triplet excitons. Furthermore, the highly twisted structure of the molecule effectively inhibits intermolecular packing, minimizing solid-state fluorescence quenching and subsequently elevating the PLQY. As illustrated in Figure 9c (molecular structures) and Figure 9d (external quantum efficiency versus current density characteristics), Device A, which is based on T-CNDF-T-*t*Cz, achieved an exceptional $EQE_{max}$ of up to 21.0%, surpassing Devices B and C, which employed molecules with fewer acceptor segments, namely, S-CNDF-S-*t*Cz and S-CNDFD-*t*Cz, respectively. Additionally, it achieved a high PLQY of up to 76% at a wavelength of 337 nm. This novel and efficient molecular design strategy presents valuable insights for future material design endeavors. In 2022, Zhang et al. [56] proposed a D-void-A structure, wherein 3,6-diphenyl-9H-carbazole (PhCz) was selected as the donor and 9H-xanthen-9-one (Xo) served as the acceptor. The donor and acceptor were connected through a void position of the acceptor, thereby avoiding the overlap of frontier orbitals and suppressing the conjugation effect. This led to a wider energy gap and blue-shifted emission. The resulting D-void-A structured molecule, 3,6-bis(3,6-diphenyl-9H-carbazol-9-yl)-9H-xanthen-9-one (33PCX) (Figure 9e), achieved a high PLQY of 92% with a peak emission at approximately 440 nm. OLED devices based on 33PCX as the emitter demonstrated a maximum EQE of 27.5% (Figure 9f) and maintained an efficiency of 27.3% at a luminance of 100 cd m$^{-2}$, providing novel insights and methodologies for the development of highly efficient blue OLEDs.

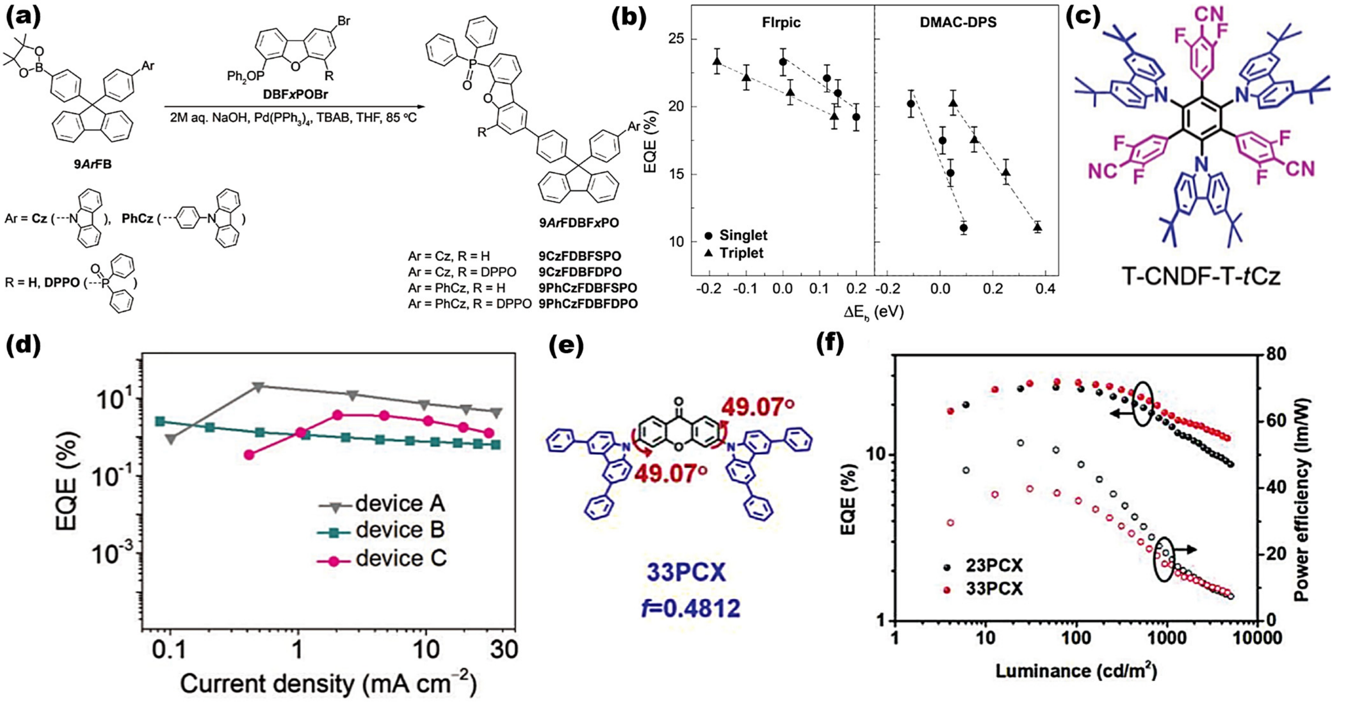

**Figure 9.** (**a**) Synthetic procedure and chemical structures of 9ArFDBFxPO. (**b**) Relationship between the maximum EQE of 9ArFDBFxPO-hosted blue OLEDs and the $\Delta E_b$ S (circle symbols) and $\Delta E_b$ T (triangle symbols) between 9ArFDBFxPO and the blue emitters [54]. (**c**) Molecular structures. (**d**) EQE–current density characteristics of Devices A, B, and C [55]. (**e**) Molecular structure of 33PCX. (**f**) EQE–luminance and PE–luminance curves of the devices. The circles and arrows indicate that the upper curve is the EQE–luminance curve, while the lower curve is the PE–luminance curve [56]. (**a**,**b**): Reprinted from [54], Copyright (2020), with permission from Elsevier.

MR-TADF molecular design is a key strategy for improving the luminescence efficiency and performance in OLED technology. It aims to optimize the performance of OLED devices by modulating the electronic structure and excited-state properties of the molecules through multiple resonance effects within the molecules [57]. In 2020, Cui and co-workers [58] designed and synthesized a novel multiple-resonance-induced MR-TADF molecule, 5Cz-TRZ ($9,9',9'',9''',9''''$ (6-(4,6-di-henyl-1,3,5-triazine-2-yl)benzene-1,2,3,4,5-pentayl) pentakis(9H-carbazole)) (depicted in Figure 10a), featuring multiple carbazole donor (Cz) units and a triazine acceptor (TRZ) moiety. By incorporating additional donor units, this molecule achieves modulation of the charge-transfer state, facilitating the RISC process with a kRISC significantly exceeding that of other classical TADF materials. As shown in Figure 10b, Device A, with Cz-TRZ doped in mCBP as the emissive layer, exhibits a maximum EQE of 29.3%, outperforming Device B utilizing TmCz-TRZ as the emitter and Device C employing DACT-II as the emitter. Furthermore, Device A demonstrates a low efficiency roll-off of less than 2.3% at 1000 cd $m^{-2}$, providing insights into the design of efficient organic molecules.

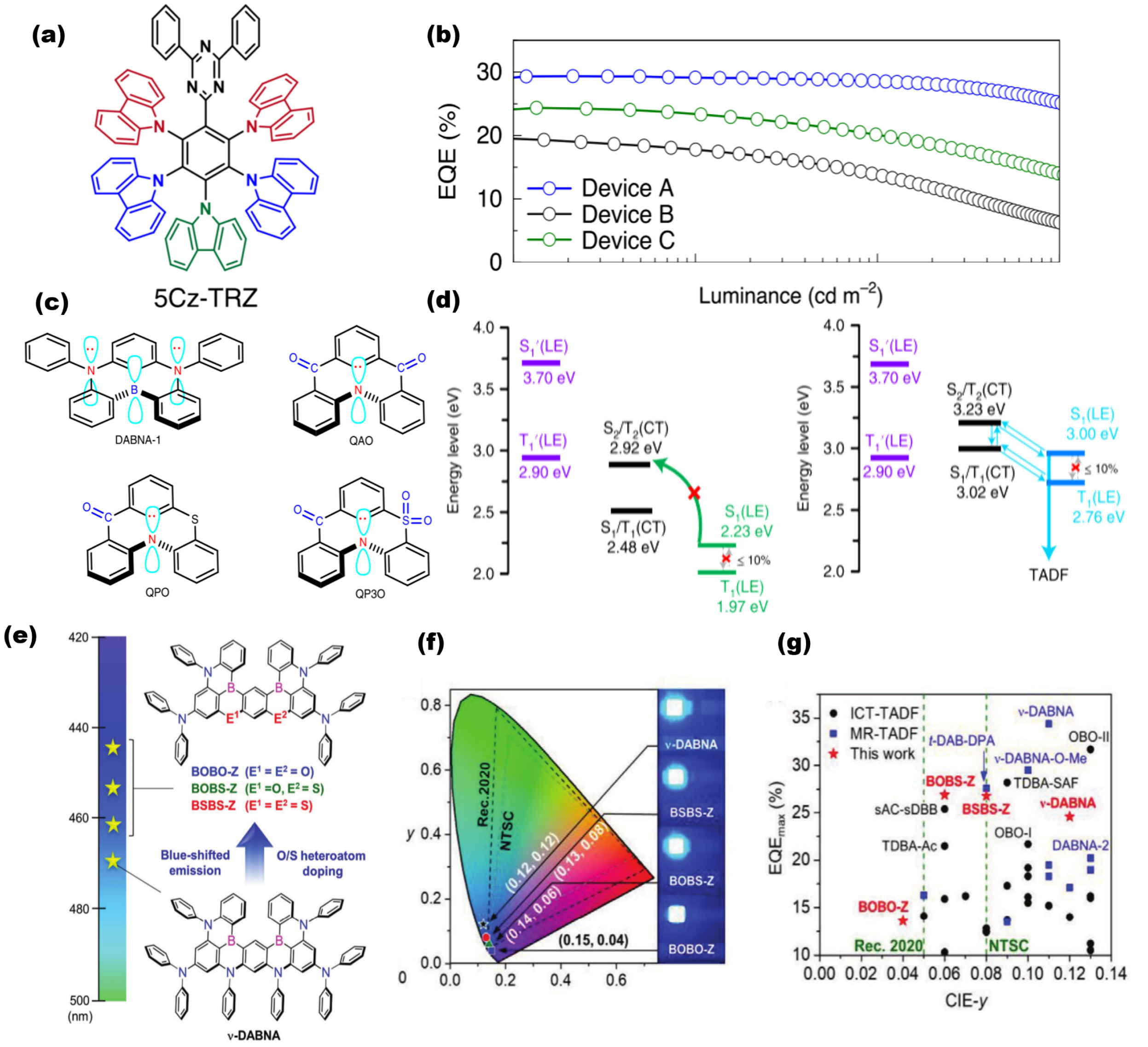

**Figure 10.** (**a**) Chemical structure of 5Cz-TRZ. (**b**) EQE versus luminance characteristics [58]. (**c**) The molecular structures of the known MR-TADF molecules DABNA-1 and QAO and the newly synthesized molecules QPO and QP3O. (**d**) Schematic depiction of state energy alignment presented for both QPO and QP3O in combination with mCP [59]. (**e**) Design for ultrapure-blue MR-TADF emitters based on polycyclo-heteraborins doped with multiple heteroatoms. (**f**) EL emission images and their color coordinates plotted in a CIE diagram. (**g**) Comparison of EL performances for the present and reported representative deep-blue OLEDs with the $EQE_{max} \geq 10\%$ and $CIE_y \leq 0.13$ [60]. (**a**,**b**): Reprinted from [58], reproduced with permission from SNCSC. (**c**,**d**): Reprinted from [59], reproduced with permission from SNCSC. (**e**–**g**): Reprinted from [60], Copyright (2022), with permission from WILEY.

In 2021, Wu et al. [59] conducted a study on the distinctive behaviors of MR-TADF materials when integrated into different host environments. They selected well-known MR-TADF compounds, specifically 5,9-diphenyl-5,9-diaza-13b-boranaphtho[3,2,1-de]anthracene (DABNA-1) and quinolino[3,2,1-de]acridine-5,9-dione (QAO). In addition, they included newly synthesized MR-TADF compounds, such as 9H-quinolino[3,2,1-kl]phenothiazin-9-one (QPO) and 9H-quinolino[3,2,1-kl]phenothiazin-9-one 5,5-dioxide (QP3O). These materials were incorporated into various host matrices, including mCBP and DPEPO, to examine the resulting effects on their performance (the molecular structures of these MR materials are shown in Figure 10c). Using DABNA-1 as an example, they discovered that in standard solutions or polystyrene-film environments, DABNA-1 did not exhibit TADF. However, when incorporated into a specific mCBP host material, DABNA-1 displayed a pronounced TADF effect. Further analysis revealed a unique interaction between DABNA-1 and mCBP, which enhanced the TADF phenomenon. Conversely, no such interaction was observed between DABNA-1 and DPEPO, resulting in the absence of the TADF effect in this host material. Figure 10d demonstrates the influence of intermolecular interactions and energy level alignments on the TADF phenomenon when different molecules (QP3O and QPO) are blended with the host material mCP. The interaction and energy level alignment between QP3O and mCP may be more conducive to the formation of thermally accessible exciplexes, thereby supporting the generation of TADF. In contrast, the interaction and energy level alignment between QPO and mCP may hinder the formation of exciplexes, or even if formed, the $\Delta E_{ST}$ may be too large, preventing the observation of TADF. This underscores the critical importance of selecting appropriate host materials for achieving efficient blue OLEDs. This study not only explained the behavioral differences in MR-TADF materials but also provided a new perspective for the development of OLED technology. In 2022, Park et al. [60] investigated ultra-narrowband and ultrapure-blue OLEDs based on polycyclic heteroboron MR-TADF emitters. To achieve this goal, the researchers designed and synthesized three novel MR-TADF materials: BOBO-Z, BOBS-Z, and BSBS-Z (Figure 10e), incorporating a multi-layer device architecture. Through precise doping with heteroatoms, these materials enabled precise tuning of the emission color while maintaining narrow bandwidths and high quantum efficiencies. OLED devices utilizing sulfur-doped BOBS-Z and BSBS-Z as the emissive layers achieved remarkable maximum external electroluminescence (EL) quantum efficiencies of 26.9% and 26.8%, respectively. Furthermore, by enhancing the light outcoupling efficiency, the bottom-emission OLEDs based on BOBO-Z, BOBS-Z, and BSBS-Z not only exhibited excellent color saturation but also achieved $EQE_{max}$ values of 16.6%, 33.1%, and 32.2%, respectively (Figure 10f,g).

In terms of energy transfer mechanisms, researchers have extensively the impact of intramolecular charge-transfer (CT) properties on the RISC process. For example, in 2020, Zhang et al. [61] achieved blue-shifted blue emission by designing and synthesizing the TADF sensitizer p4TCzPhBN, which is based on multiple donor–acceptor (Ds-As) carbazole-biphenylnitrile (CzPhBN) derivatives. They reduced the $\Delta E_{ST}$ and enhanced the RISC rate by introducing a weak acceptor cyanophenyl (PhCN) unit to replace the original strong acceptor cyano (CN) unit. As illustrated in Figure 11a,b, when p4TCzPhBN was used as a sensitizer for t-DABNA, the OLED device achieved a maximum EQE of 32.5%, signifying a significant improvement in both efficiency and stability for blue OLEDs. Additionally, in 2021, Jeon et al. [20] successfully synthesized two novel TADF materials, PPCzTrz and PCzTrz (shown in Figure 11c), and integrated these materials with the previously reported deep-blue emitter ν-DABNA for use in a triplet-exciton-distributed TADF (TED-TADF) device architecture based on a triplet-exciton recycling protocol (as depicted in Figure 11d). This protocol enhances the conversion efficiency from triplet excitons to singlet excitons by facilitating the RISC process, thereby maximizing the utilization of exciton energy. The blue OLEDs utilizing these novel materials and device strategies achieved a maximum EQE of nearly 33.5% (Figure 11e), maintaining an EQE of approximately 23.8% even at a brightness of 1000 cd $m^{-2}$. This represents a significant advancement towards the commercialization of deep-blue OLEDs. In 2022, Bian et al. [62] synthesized a novel ambipolar self-hosted TADF material, tCBNDADPO, whose chemical structure and fundamental physical properties are depicted in Figure 11f. By accelerating the singlet radiative rate, suppressing non-radiative transitions, and optimizing the doping concentration, they significantly enhanced the singlet radiative rate constant while effectively inhibiting both singlet and triplet non-radiative transitions. This optimization of the energy transfer process ensures that radiative transitions dominate the emission process. At a doping concentration of 30%, the material achieved an EQE of 30.8% (Figure 11g), demonstrating the feasibility of the ambipolar self-hosting strategy in constructing practically applicable MR materials.

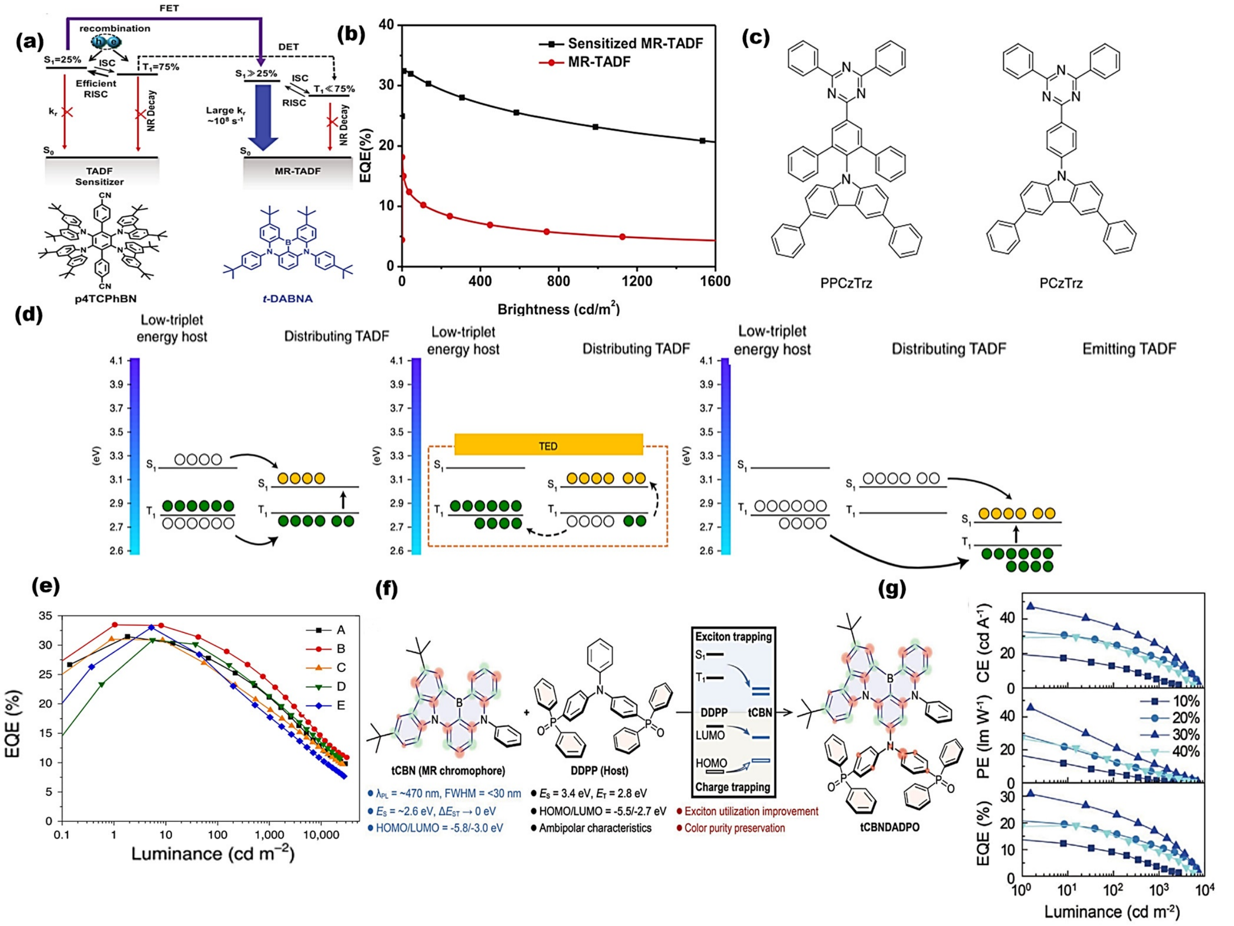

**Figure 11.** (**a**) Energy transfer process in the sensitizing system. (**b**) EQE–brightness curves [61]. (**c**) Chemical structures of PPCzTrz and PCzTrz. (**d**) Emission mechanism of TED-TADF. (**e**) EQE versus luminance characteristics. A, TADF (10 wt%):ν-DABNA (0.5 wt%); B, TADF (10 wt%):ν-DABNA (1.0 wt%); C, TADF (20 wt%):ν-DABNA (0.5 wt%); D, TADF (20 wt%):ν-DABNA (1.0 wt%); E, ν-DABNA (1.0 wt%) [20]. (**f**) Chemical structures and basic physical properties. (**g**) Dependence of efficiencies versus luminance curves on x% [62]. (**a**,**b**): Reprinted from [61], Copyright (2020), with permission from WILEY. (**c**–**e**): Reprinted from [20], reproduced with permission from SNCSC. (**f**,**g**): Reprinted from [62], Copyright (2022), with permission from WILEY.

In recent years, HF OLED technology has provided a new direction for the development of blue OLEDs. In 2021, Braveenth et al. [63] synthesized two deep-blue TADF materials, DBA–BFICz and DBA–BTICz (Figure 12a), by combining an oxygen-bridged boron (DBA) acceptor with heteroatom-based donors (BFICz and BTICz) containing oxygen and sulfur, respectively. As depicted in Figure 12b, when DBA–BFICz served as the TADF sensitizing host and ν-DABNA was utilized as the fluorescent dopant in an HF OLED device, a maximum EQE of up to 38.8% was achieved, demonstrating high efficiency and narrow-bandwidth light-emitting performance. In 2023,Lee et al. [64] designed and synthesized highly efficient quadrupolar D-A-D structured TADF sensitizers, namely, 3,11-bis(5-phenylindolo[3,2-a]carbazol-12(5H)-yl)–5,9-dioxa-13b-boranaphtho[3,2,1-de]anthracene (DBA-DmICz) and 3,11-bis(1,3,6,8-tetramethyl-9H-carbazol-9-yl)–5,9-dioxa-13b-boranaphtho[3,2,1-de]anthracene (DBA-DTMCz) (Figure 12c). By suppressing the

DET process and enhancing the Förster resonance energy transfer (FRET) process, they successfully improved the exciton utilization efficiency and color purity of the HF system. As depicted in Figure 12d, the TADF OLEDs based on DBA-DmICz and DBA-DTMCz achieved $EQE_{max}$ values of 31.6% and 37.0%, respectively. The HF device fabricated with DBA-DTMCz in conjunction with ν-DABNA attained an outstanding $EQE_{max}$ of 43.9%, accompanied by a low efficiency roll-off. This will help in the subsequent development of HF OLED materials. In 2024, Stavrou et al. [65] demonstrated a comprehensive study by contrasting the device performances of different TADF sensitizers, including spiro-linked TADF molecule ACRSA, DMAC-TRZ, and AZB-TRZ, combined with various terminal emitters, particularly ν-DABNA (Figure 12e–g). Their findings revealed that the rigid structure of spiro-linked ACRSA molecules effectively suppresses dihedral-angle inhomogeneity, enabling efficient FRET, resulting in nearly 100% FRET efficiency and a substantial enhancement of EQE in blue HF-OLEDs. This research underscores a potential misconception about the over-reliance on ostensibly optimal TADF materials, such as DMAC-TRZ, as sensitizers, neglecting the exploration of alternative, highly efficient combinations. It is worth noting that even a seemingly less favorable TADF sensitizer like ACRSA was found to possess untapped potential. For instance, incorporating just 1 wt% of ν-DABNA into ACRSA-based devices led to a significant increase in $EQE_{max}$ to 28.5%. By re-evaluating and adjusting the application strategies of these materials in HF-OLEDs, this study opens new avenues for discovering material combinations that can significantly enhance the performance of blue HF-OLEDs.

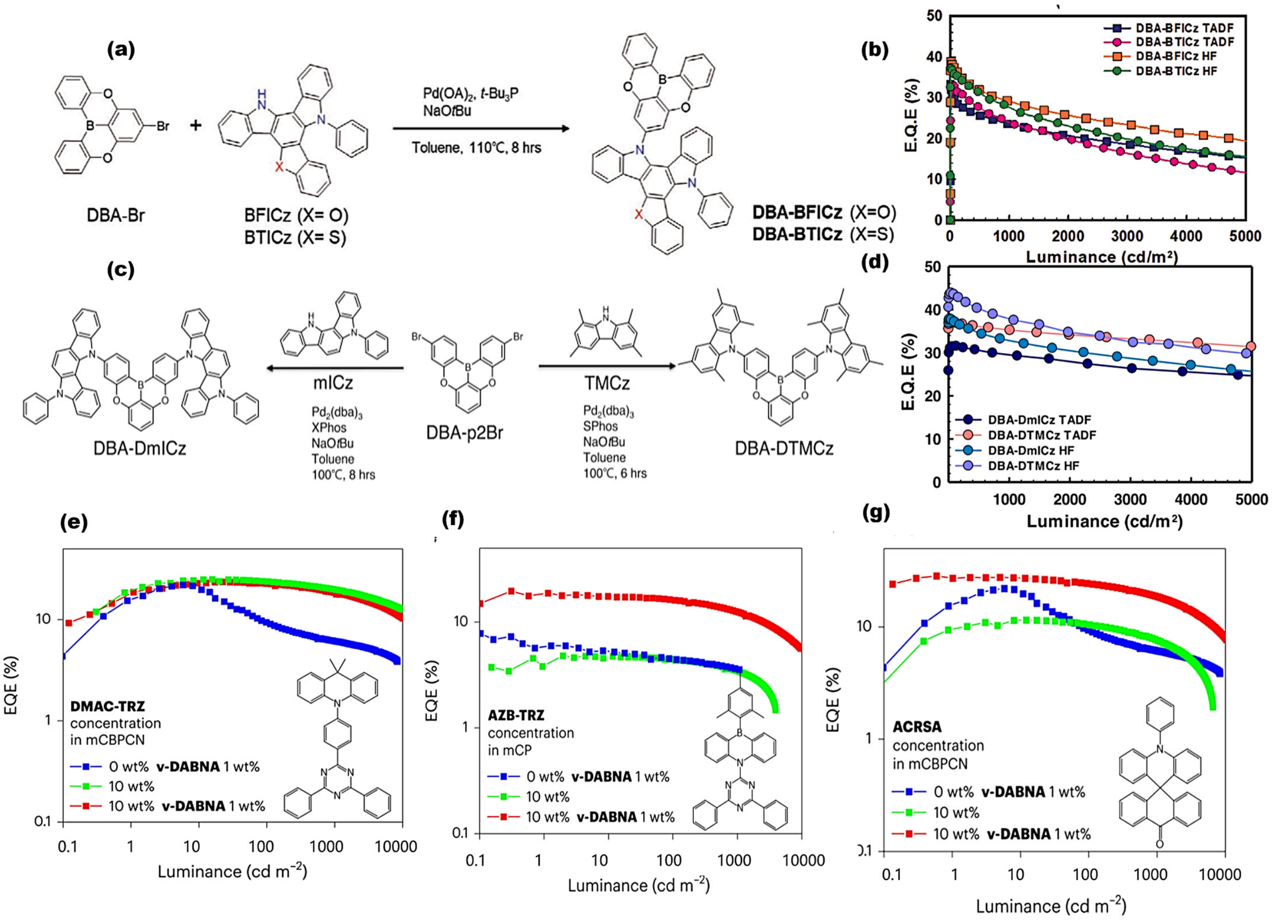

**Figure 12.** (**a**) Synthetic procedure of DBA-BFICz and DBA-BTICz. (**b**) EQE versus luminescence [63]. (**c**) Synthetic routes for DBA-DmICz and DBA-DTMCz. (**d**) EQE versus luminance. (**e**) EQE versus luminance of DMAC-TRZ OLEDs [64]. (**f**) EQE versus luminance of AZB-TRZ OLEDs. (**g**) EQE versus luminance of ACRSA OLEDs [65]. (**a**,**b**): Reprinted from [63], Copyright (2021), with permission from WILEY.

## 4. Challenges and Perspectives

Despite the significant progress made in improving the luminous efficiency and stability of blue OLEDs through the development of fluorescent, phosphorescent, and TADF materials, their commercialization still faces several daunting challenges. To provide a more intuitive comparison, the performance of most of the blue OLED materials mentioned above is summarized in Table 1.

**Table 1.** Device performance of blue OLED materials.

| Type | Materials | EQE$_{max}$ | Initial Luminescence/(cd m$^{-2}$) | Lifetime/h | CIE(x,y) | Ref. |
|---|---|---|---|---|---|---|
| Fluorescent | DP | 6.4 | - | - | (0.153, 0.087) | [36] |
| Fluorescent | SP | 11.3 | - | - | (0.158, 0.068) | [36] |
| Fluorescent | SAFPI-2 | 3.83 | - | - | (0.15, 0.10) | [37] |
| Fluorescent | SAFPI-3 | 4.99 | - | - | (0.16, 0.17) | [37] |
| Fluorescent | $Zn(PhCzKt)_2$ | 1.54 | - | - | (0.1558, 0.0901) | [39] |
| Fluorescent | Zn-1 | 3.2 | - | - | (0.16, 0.09) | [40] |
| Fluorescent | Zn-2 | 1.4 | - | - | (0.18, 0.11) | [40] |
| Fluorescent | PAC | 10.48 | - | - | (0.15, 0.13) | [17] |
| Fluorescent | 2FPPICz, PAC | 9.14 | - | - | (0.15, 0.17) | [41] |
| Fluorescent | PITPh | 6.1 | - | - | (0.16, 0.06) | [42] |
| Fluorescent | PPITPh | 11.83 | - | - | (0.15, 0.07) | [42] |
| Phosphorescent | 1-mtp-SBF | 25.6 | - | - | (0.14, 0.32) | [45] |
| Phosphorescent | PtON-tb-DTB | 20.9 | 1200 | LT$_{95}$ = 169.3 | (0.14, 0.22) | [47] |
| Phosphorescent | PtON-tb-TTB | 26.3 | 1200 | LT$_{95}$ = 31 | (0.14, 0.22) | [47] |
| Phosphorescent | FIrpic | 12.7 | - | - | - | [30] |
| Phosphorescent | $Ir(cb)_3$ | 21.6 | - | - | - | [49] |
| Phosphorescent | PtON7-dtb(TBPDP as emitter) | 16.9 | 1000 | LT$_{50}$ = 192.2 h | (0.109, 0.134) | [50] |
| Phosphorescent | PtON7-dtb(ν-DABNA as emitter) | 32.2 | 1000 | LT$_{50}$ = 253.8 | (0.115, 0.091) | [50] |
| Phosphorescent | B–4–TMS | 33.43 | 100 | LT$_{50}$ = 4465 | (0.119, 0.123) | [51] |
| Phosphorescent | B–5–TMS | 33.42 | 100 | LT$_{50}$ = 4552 | (0.119, 0.123) | [51] |
| TADF | TMCz-BO | 20.7 | - | - | (0.14, 0.18) | [52] |
| TADF | m-ν-DABNA | 36.2 | - | - | (0.12, 0.12) | [53] |
| TADF | 4F-ν-DABNA | 35.8 | - | - | (0.13, 0.08) | [53] |
| TADF | 4F-m-ν-DABNA | 33.7 | - | - | (0.13, 0.06) | [53] |
| TADF | HDT-1 | 41 | 1000 | LT$_{95}$ = 18 | (0.13, 0.16) | [19] |
| TADF | DMAC-DPS | 11.1 | - | - | - | [30] |
| Phosphorescent | 9CzFDBFDPO(FIRPIC as emitter) | 23.3 | - | - | (0.16, 0.31) | [54] |
| TADF | 9CzFDBFDPO(DMAC-DPS as emitter) | 20.2 | - |  | (0.18, 0.22) | [54] |
| TADF | T-CNDF-T-t Cz | 21.0 | - | - | (0.19, 0.35) | [55] |
| TADF | 23PCX | 25.5 | 100 | LT$_{95}$ = 750 | (0.176, 0.357) | [56] |
| TADF | 33PCX | 27.5 | 100 | LT$_{95}$ = 650 | (0.156, 0.252) | [56] |
| TADF | 5Cz-TRZ | 29.3 | 1000 | LT$_{90}$ = 600 | - | [58] |
| TADF | BOBO-Z | 16.6 |  | - | (0.15, 0.04) | [60] |
| TADF | BOBS-Z | 33.1 | - | - | (0.14, 0.06) | [60] |
| TADF | BSBS-Z | 32.2 | - | - | (0.13, 0.08) | [60] |
| TADF | p4TCzPhBN | 32.5 | 1000 | LT$_{80}$ > 20 | CIE$_y$ = 0.12 | [61] |
| TADF | PPCzTrz, PCzTrz | 33.5 | 1000 | LT$_{50}$ > 5000 | (0.12, 0.09) | [20] |
| TADF | tCBNDADPO | 30.8 | - | - | (0.14, 0.22) | [62] |
| TADF | DBA-BFICz | 38.8 | - | - | (0.12, 0.15) | [63] |
| TADF | DBA-DTMCz | 43.9 | - | - | (0.12, 0.16) | [64] |
| TADF | ACRSA | 28.5 | - | - | - | [65] |

In fluorescent materials, the inherent limitations of the RISC process efficiency and IQE, which is approximately 25%, restrict their performance potential. Despite the development of numerous novel molecular structures and device designs, their maximum efficiency, even for the most advanced fluorescent materials, typically only reaches around 10%. In contrast, phosphorescent materials can achieve efficiencies up to 30%, and TADF materials can reach efficiencies of up to 40%. Furthermore, the scarcity of short-wavelength materials limits the expansion of color gamut and improvement in color purity. The design of phosphorescent materials is relatively challenging, and they face issues of device degradation, leading to shortened lifetime, insufficient color purity, and poor triplet-exciton capture efficiency. Additionally, the heavy metals Ir and Pt used in phosphorescent materials are costly and environmentally unfriendly. In recent years, researchers have been actively exploring low-cost, low-toxicity phosphorescent complexes, such as those with rare earth elements like cerium and europium. Although TADF materials exhibit great potential, the synthesis of high-efficiency materials is complex and costly. Further exploration is necessary in terms of energy transfer efficiency, device structure optimization, efficiency roll-off at high brightness, and exciton lifetime, to maintain high efficiency while achieving narrower emission bandwidths and higher color purity. While MR TADF materials can address the issue of insufficient color purity caused by the excessively large FWHM of traditional D-A TADF materials, they rarely reach the deep-blue region. MR-TADF materials require further improvements in color purity and efficiency, as well as the preparation of low-concentration doped devices, to enable their commercialization [17,19,20,30–65].

Despite the numerous challenges faced by blue OLED materials, researchers continue to explore new material design strategies to address these issues. Table 2 lists several high-performance materials introduced in this paper along with their characteristics. For fluorescent materials, the SP material synthesized through molecular structure design has achieved a maximum EQE of 11.3%, which is among the best in fluorescent materials. Adopting the hot exciton mechanism, the PPITPh material has achieved a maximum EQE of 11.83%, highlighting the importance of this mechanism in enhancing efficiency. Hot exciton materials significantly shorten the lifetime of nanosecond-scale triplet excitons through their rapid RISC process, preventing the accumulation of triplet excitons. This allows OLEDs to be manufactured using nondoped techniques, thereby achieving high efficiency and potential for low efficiency roll-off [17,33,41,42]. In the realm of phosphorescent and TADF materials, HF-OLED technology plays a crucial role. This technology enhances FRET by utilizing phosphorescent and TADF as separate end-emitting sensitizers, combined with high-performance deep-blue "triplet harvesting" sensitizers, significantly improving both luminous efficiency and stability. The phosphorescent material B–4–TMS, shown in Table 2, achieves a maximum EQE of over 30% when used as a sensitizer, with a lifetime ($LT_{50}$) exceeding 4000 h at an initial luminescence of 1000 cd/m$^2$. The TADF materials HDT-1 and DBA-DTMCz, when used as sensitizers, both achieve maximum EQEs of over 40%. In comparison, TADF materials as sensitizers typically exhibit superior efficiency and color purity but usually require more complex designs and may face stability issues. On the other hand, phosphorescent materials as sensitizers generally offer better stability and longer lifetimes but are more costly and have slightly lower color purity compared to TADF materials [49–51,63–65]. Additionally, the materials PPCzTrz and PCzTrz, when combined with the deep-blue emitter ν-DABNA, achieve a maximum EQE of 33.5% through cascade energy transfer and triplet-exciton harvesting mechanisms. At an initial luminance of 100 cd/m$^2$, the devices exhibit an $LT_{50}$ exceeding 5000 h. The devices demonstrate excellent performance. Although hot exciton materials and HF-OLED technology have brought blue phosphorescent and TADF materials close to commercialization, their high cost, development complexity, and potential instability may still limit their widespread application. Therefore, fluorescent materials with lower device degradation and longer overall lifetimes remain the primary choice for commercial blue OLEDs [66,67]. Nevertheless, with the advancement of new generations of materials—offering high efficiency, long lifetime, pure color, low cost, and minimal environmental impact—it is reasonable to expect that phosphorescent and TADF materials will soon enter the commercial market.

**Table 2.** Device high-performance blue OLED materials.

| Type | Materials | Mechanism | EQE$_{max}$ | Initial Luminescence/(cd m$^{-2}$) | Lifetime/h | CIE(x,y) | Ref. |
|---|---|---|---|---|---|---|---|
| Fluorescent | SP | Molecular structure design | 11.3 | - | - | (0.158, 0.068) | [36] |
| Fluorescent | PPITPh | Hot exciton | 11.83 | - | - | (0.15, 0.07) | [42] |
| Phosphorescent | PtON7-dtb (ν-DABNA as emitter) | HF-OLED | 32.2 | 1000 | $LT_{50} = 253.8$ | (0.115, 0.091) | [50] |
| Phosphorescent | B–4–TMS | HF-OLED | 33.43 | 100 | $LT_{50} = 4465$ | (0.119, 0.123) | [51] |
| Phosphorescent | B–5–TMS | HF-OLED | 33.42 | 100 | $LT_{50} = 4552$ | (0.119, 0.123) | [51] |
| TADF | HDT-1 | Two-unit-stacked tandem OLED, HF-OLED | 41 | 1000 | $LT_{95} = 18$ | (0.13, 0.16) | [19] |
| TADF | PPCzTrz, PCzTrz | Cascade energy transfer, triplet-exciton recycling | 33.5 | 1000 | $LT_{50} > 5000$ | (0.12, 0.09) | [20] |
| TADF | DBA-DTMCz | HF OLED | 43.9 | - | - | (0.12, 0.16) | [64] |

In summary, OLED technology presents a wide range of applications in the display and lighting industries. However, the luminous efficiency, durability, and material stability of blue OLEDs pose significant challenges to their development. This article examines the progress of three generations of blue OLED materials—fluorescent, phosphorescent, and TADF—and highlights the distinct advantages and limitations of each material in improving performance. By focusing on molecular design, optimizing device structure, and adopting new technologies, blue OLEDs have made notable advancements in terms of luminous efficiency, lifetime, and color accuracy. Yet, there are still hurdles that need to be overcome for full commercialization. Future advancements will concentrate on enhancing stability, managing costs, optimizing environmental sustainability, and improving color accuracy. New materials like hot exciton materials and HF OLED technology are anticipated to expedite the commercialization of OLEDs. Ultimately, blue OLEDs with high efficiency, stability, and color accuracy are poised to be extensively utilized in displays, lighting, medicine, and various other aspects of life.

**Author Contributions:** Writing original draft preparation: X.Y.; Writing review and editing: G.M. and K.W.; Funding acquisition: X.T. and G.M. All authors have read and agreed to the published version of the manuscript.

**Funding:** G.M. is sponsored by the National Natural Science Foundation of China (NSFC No. 62305022). X.T. is sponsored by the National Key R&D Program of China (2021YFA0717600), National Natural Science Foundation of China (NSFC No. 62035004, NSFC No. U22A2081), and Young Elite Scientists Sponsorship Program by CAST (No. YESS20200163).

**Institutional Review Board Statement:** Not applicable.

**Informed Consent Statement:** Not applicable.

**Data Availability Statement:** Not applicable.

**Conflicts of Interest:** The authors declare no conflicts of interest.

## References

1. Tang, C.W.; VanSlyke, S.A. Organic electroluminescent diodes. *Appl. Phys. Lett.* **1987**, *51*, 913–915. [CrossRef]
2. Kosai, S.; Badin, A.B.; Qiu, Y.; Matsubae, K.; Suh, S.; Yamasue, E. Evaluation of resource use in the household lighting sector in Malaysia considering land disturbances through mining activities. *Resour. Conserv. Recycl.* **2021**, *166*, 105343. [CrossRef]
3. Pode, R. Organic light emitting diode devices: An energy efficient solid state lighting for applications. *Renew. Sustain. Energy Rev.* **2020**, *133*, 110043. [CrossRef]

4. Nayak, D.; Choudhary, R.B. A survey of the structure, fabrication, and characterization of advanced organic light emitting diodes. *Microelectron. Reliab.* **2023**, *144*, 114959. [CrossRef]
5. Takahashi, Y.; Furuki, Y.; Yoshida, S.; Otani, T.; Muto, M.; Suga, Y.; Ito, Y. 29.1: A New Achromatic Quarter-Wave Film Using Liquid-Crystal Materials for Anti-Reflection of OLEDs. *Dig. Tech. Pap. SID Int. Symp.* **2014**, *45*, 381–384. [CrossRef]
6. Cinquino, M.; Prontera, C.T.; Pugliese, M.; Giannuzzi, R.; Taurino, D.; Gigli, G.; Maiorano, V. Light-emitting textiles: Device architectures, working principles, and applications. *Micromachines* **2021**, *12*, 652. [CrossRef]
7. Hong, G.; Gan, X.; Leonhardt, C.; Zhang, Z.; Seibert, J.; Busch, J.M.; Bräse, S. A brief history of OLEDs—Emitter development and industry milestones. *Adv. Mater.* **2021**, *33*, 2005630. [CrossRef]
8. Huang, Y.; Hsiang, E.L.; Deng, M.Y.; Wu, S.T. Mini-LED, Micro-LED and OLED displays: Present status and future perspectives. *Light Sci. Appl.* **2020**, *9*, 105. [CrossRef]
9. Jang, H.J.; Lee, J.Y.; Baek, G.W.; Kwak, J.; Park, J.H. Progress in the development of the display performance of AR, VR, QLED and OLED devices in recent years. *J. Inf. Disp.* **2022**, *23*, 1–17. [CrossRef]
10. Murawski, C.; Gather, M.C. Emerging biomedical applications of organic light-emitting diodes. *Adv. Opt. Mater.* **2021**, *9*, 2100269. [CrossRef]
11. Song, J.; Lee, H.; Jeong, E.G.; Choi, K.C.; Yoo, S. Organic light-emitting diodes: Pushing toward the limits and beyond. *Adv. Mater.* **2020**, *32*, 1907539. [CrossRef] [PubMed]
12. Matarèse, B.F.E. Embryonic development of fully biocompatible organic light-emitting diodes. In Proceedings of the 2021 IEEE 21st International Conference on Nanotechnology (NANO), Montréal, QC, Canada, 28–30 July 2021.
13. Kim, D.; Yokota, T.; Suzuki, T.; Lee, S.; Woo, T.; Yukita, W.; Koizumi, M.; Tachibana, Y.; Yawo, H.; Onodera, H. Ultraflexible organic light-emitting diodes for optogenetic nerve stimulation. *Proc. Natl. Acad. Sci. USA* **2020**, *117*, 21138–21146. [CrossRef] [PubMed]
14. Siddiqui, I.; Kumar, S.; Tsai, Y.F.; Gautam, P.; Shahnawaz; Kesavan, K.; Lin, J.T.; Khai, L.; Chou, K.H.; Choudhury, A. Status and challenges of blue OLEDs: A review. *Nanomaterials* **2023**, *13*, 2521. [CrossRef] [PubMed]
15. Kagatikar, S.; Sunil, D. A systematic review on 1, 8-naphthalimide derivatives as emissive materials in organic light-emitting diodes. *J. Mater. Sci.* **2022**, *57*, 105–139. [CrossRef]
16. Xie, M.; Sun, M.; Xue, S.; Yang, W. Recent progress of blue fluorescent organic light-emitting diodes with narrow full width at half maximum. *Dye Pigment.* **2023**, *208*, 110799. [CrossRef]
17. Xu, Y.; Liang, X.; Zhou, X.; Yuan, P.; Zhou, J.; Wang, C.; Li, B.; Hu, D.; Qiao, X.; Jiang, X. Highly efficient blue fluorescent OLEDs based on upper level triplet–singlet intersystem crossing. *Adv. Mater.* **2019**, *31*, 1807388. [CrossRef]
18. Sudheendran, S.S.; Dubey, D.K.; Shahnawaz; Yadav, R.A.K.; Nagar, M.R.; Sharma, A.; Tung, F.C.; Jou, J.H. Approaches for long lifetime organic light emitting diodes. *Adv. Sci.* **2021**, *8*, 2002254. [CrossRef]
19. Chan, C.Y.; Tanaka, M.; Lee, Y.T.; Wong, Y.W.; Nakanotani, H.; Hatakeyama, T.; Adachi, C. Stable pure-blue hyperfluorescence organic light-emitting diodes with high-efficiency and narrow emission. *Nat. Photonics* **2021**, *15*, 203–207. [CrossRef]
20. Jeon, S.O.; Lee, K.H.; Kim, J.S.; Ihn, S.G.; Chung, Y.S.; Kim, J.W.; Lee, H.; Kim, S.; Choi, H.; Lee, J.Y. High-efficiency, long-lifetime deep-blue organic light-emitting diodes. *Nat. Photonics* **2021**, *15*, 208–215. [CrossRef]
21. Sun, J.; Ahn, H.; Kang, S.; Ko, S.B.; Song, D.; Um, H.A.; Kim, S.; Lee, Y.; Jeon, P.; Hwang, S.H. Exceptionally stable blue phosphorescent organic light-emitting diodes. *Nat. Photonics* **2022**, *16*, 212–218. [CrossRef]
22. Corrêa Santos, D.; Vieira Marques, M.d.F. Blue light polymeric emitters for the development of OLED devices. *J. Mater. Sci. Mater. Electron.* **2022**, *33*, 12529–12565. [CrossRef]
23. Li, L.; Zhu, X.; Sun, S.; Zhang, C.; Yang, B.; Liu, S.; Liu, Z. Blue Organic Light Emitting Diode Materials based on Different Light-emitting Groups. *Curr. Org. Chem.* **2023**, *27*, 352–362. [CrossRef]
24. Kalyani, N.T.; Dhoble, S.J. Organic light emitting diodes: Energy saving lighting technology—A review. *Renew. Sustain. Energy Rev.* **2012**, *16*, 2696–2723. [CrossRef]
25. Wang, S.; Zhang, H.; Zhang, B.; Xie, Z.; Wong, W.Y. Towards high-power-efficiency solution-processed OLEDs: Material and device perspectives. *Mater. Sci. Eng. R Rep.* **2020**, *140*, 100547. [CrossRef]
26. Huang, J.; Su, J.H.; Tian, H. The development of anthracene derivatives for organic light-emitting diodes. *J. Mater. Chem.* **2012**, *22*, 10977–10989. [CrossRef]
27. Adachi, C.; Baldo, M.A.; Thompson, M.E.; Forrest, S.R. Nearly 100% internal phosphorescence efficiency in an organic light-emitting device. *J. Appl. Phys.* **2001**, *90*, 5048–5051. [CrossRef]
28. Lee, J.H.; Chen, C.H.; Lee, P.H.; Lin, H.Y.; Leung, M.k.; Chiu, T.L.; Lin, C.F. Blue organic light-emitting diodes: Current status, challenges, and future outlook. *J. Mater. Chem. C* **2019**, *7*, 5874–5888. [CrossRef]
29. Zhang, Q.; Li, J.; Shizu, K.; Huang, S.; Hirata, S.; Miyazaki, H.; Adachi, C. Design of efficient thermally activated delayed fluorescence materials for pure blue organic light emitting diodes. *J. Am. Chem. Soc.* **2012**, *134*, 14706–14709. [CrossRef]
30. Jang, E.B.; Choi, G.S.; Bae, E.J.; Ju, B.K.; Park, Y.W. Doping-Free Phosphorescent and Thermally Activated Delayed Fluorescent Organic Light-Emitting Diodes with an Ultra-Thin Emission Layer. *Nanomaterials* **2023**, *13*, 2366. [CrossRef]
31. Köhler, A.; Bässler, H. *Electronic Processes in Organic Semiconductors: An Introduction*; John Wiley & Sons: Weinheim, Germany, 2015; pp. 362–365.
32. Tankelevičiūtė, E.; Samuel, I.D.W.; Zysman-Colman, E. The Blue Problem: OLED Stability and Degradation Mechanisms. *J. Phys. Chem. Lett.* **2024**, *15*, 1034–1047. [CrossRef]

33. Park, S.W.; Kim, D.; Rhee, Y.M. Overcoming the limitation of spin statistics in organic light emitting diodes (OLEDs): Hot exciton mechanism and its characterization. *Int. J. Mol. Sci.* **2023**, *24*, 12362. [CrossRef] [PubMed]
34. Sun, J.; Zhang, H.; Feng, X.; Tian, M.; Yang, D.; He, H.; Liu, K.; Li, J. Three times lifetime improvement of red-emitting organic light-emitting diodes based on bipolar host material. *ECS J. Solid State Sci. Technol.* **2018**, *7*, R57. [CrossRef]
35. Zhao, N.; Li, Z.; Qin, L.; Cui, Z.; Sun, Z.; Cheng, Z.; Jiang, C.; Wang, S.; Zhao, T.; Liao, Y. Lifetime measurement and aging mechanism analysis of OLED subpixels. *Displays* **2022**, *75*, 102326. [CrossRef]
36. Xiao, S.; Gao, Y.; Wang, R.; Liu, H.; Li, W.; Zhou, C.; Xue, S.; Zhang, S.T.; Yang, B.; Ma, Y. Highly efficient hybridized local and Charge-transfer (HLCT) Deep-blue electroluminescence with excellent molecular horizontal orientation. *Chem. Eng. J.* **2022**, *440*, 135911. [CrossRef]
37. Chen, S.W.; Chen, J.X.; Chen, G.; Gong, Y.; Liu, B.; Chen, Y.; Jin, J.M.; Wang, R.; Wang, R.J.; Liu, J. Versatile deep blue fluorescent materials based on the hybridization of phenanthroimidazole and fluorene derivatives. *Dye Pigment.* **2024**, *222*, 111829. [CrossRef]
38. Rashamuse, T.J.; Mohlala, R.L.; Coyanis, E.M.; Magwa, N.P. A review: Blue fluorescent Zinc (II) complexes for OLEDs—A last five-year recap. *Molecules* **2023**, *28*, 5272. [CrossRef]
39. Liu, J.; Li, H.L.; Ma, D.G.; Gong, Y.Y.; Jiang, M.H.; Li, S.G.; Jin, B. Efficient deep-blue electroluminescent devices based on a novel β-diketone zinc complex. *Inorganica Chim. Acta* **2022**, *542*, 121134. [CrossRef]
40. Solanki, J.D.; Siddiqui, I.; Gautam, P.; Gupta, V.K.; Jou, J.H.; Surati, K.R. Blue fluorescent Zinc (II) complexes bearing schiff base ligand for solution-processed organic light-emitting diodes with $\mathrm{CIE_y} \leq 0.09$. *Opt. Mater.* **2022**, *134*, 113222. [CrossRef]
41. Yang, J.; Hu, D.; Zhu, F.; Ma, Y.; Yan, D. High-efficiency blue-emission crystalline organic light-emitting diodes sensitized by "hot exciton" fluorescent nanoaggregates. *Sci. Adv.* **2022**, *8*, eadd1757. [CrossRef]
42. Du, C.; Liu, H.; Cheng, Z.; Zhang, S.; Qu, Z.; Yang, D.; Qiao, X.; Zhao, Z.; Lu, P. Ultraefficient Non-Doped Deep Blue Fluorescent OLED: Achieving a High EQE of 10.17% at 1000 cd $\mathrm{m}^{-2}$ with $\mathrm{CIE_y} < 0.08$. *Adv. Funct. Mater.* **2023**, *33*, 2304854.
43. Feng, H.T.; Zeng, J.; Yin, P.A.; Wang, X.D.; Peng, Q.; Zhao, Z.; Lam, J.W.Y.; Tang, B.Z. Tuning molecular emission of organic emitters from fluorescence to phosphorescence through push-pull electronic effects. *Nat. Commun.* **2020**, *11*, 2617. [CrossRef] [PubMed]
44. Ye, W.; Ma, H.; Shi, H.; Wang, H.; Lv, A.; Bian, L.; Zhang, M.; Ma, C.; Ling, K.; Gu, M. Confining isolated chromophores for highly efficient blue phosphorescence. *Nat. Mater.* **2021**, *20*, 1539–1544. [CrossRef] [PubMed]
45. Kong, F.C.; Zhang, Y.L.; Quinton, C.; McIntosh, N.; Yang, S.Y.; Rault-Berthelot, J.; Lucas, F.; Brouillac, C.; Jeannin, O.; Cornil, J. Pure Hydrocarbon Materials as Highly Efficient Host for White Phosphorescent Organic Light-Emitting Diodes: A New Molecular Design Approach. *Angew. Chem. Int. Ed.* **2022**, *61*, e202207204. [CrossRef] [PubMed]
46. Zhou, Y.; Song, D.; Zhao, S.; Qiao, B.; Ning, Y.; Dong, J.; Xu, Z. Small dose of phosphorescent dopant enabling high efficiency and bright solution-processed sky-blue organic light-emitting diodes. *Opt. Mater.* **2022**, *128*, 112278. [CrossRef]
47. Jung, Y.H.; Lee, G.S.; Muruganantham, S.; Kim, H.R.; Oh, J.H.; Ham, J.H.; Yadav, S.B.; Lee, J.H.; Chae, M.Y.; Kim, Y.-H. Modified t-butyl in tetradentate platinum (II) complexes enables exceptional lifetime for blue-phosphorescent organic light-emitting diodes. *Nat. Commun.* **2024**, *15*, 2977. [CrossRef]
48. Trindade, G.F.; Sul, S.; Kim, J.; Havelund, R.; Eyres, A.; Park, S.; Shin, Y.; Bae, H.J.; Sung, Y.M.; Matjacic, L. Direct identification of interfacial degradation in blue OLEDs using nanoscale chemical depth profiling. *Nat. Commun.* **2023**, *14*, 8066. [CrossRef]
49. Lee, H.; Hwang, K.M.; Kim, K.J.; Song, Y.N.; Kim, Y.K.; Kim, T. Effects of the phosphorescent sensitizer on charge dynamics in deep blue phosphor-sensitized-fluorescent organic light-emitting diodes. *J. Inf. Disp.* **2022**, *23*, 97–103. [CrossRef]
50. Nam, S.; Kim, J.W.; Bae, H.J.; Maruyama, Y.M.; Jeong, D.; Kim, J.; Kim, J.S.; Son, W.J.; Jeong, H.; Lee, J. Improved efficiency and lifetime of deep-blue hyperfluorescent organic light-emitting diode using Pt (II) complex as phosphorescent sensitizer. *Adv. Sci.* **2021**, *8*, 2100586. [CrossRef]
51. Wu, C.; Tong, K.N.; Shi, K.; Jin, Z.; Wu, Y.; Mu, Y.; Huo, Y.; Tang, M.C.; Yang, C.; Meng, H. New [3+ 2+ 1] Iridium Complexes as Effective Phosphorescent Sensitizers for Efficient Narrowband Saturated–Blue Hyper–OLEDs. *Adv. Sci.* **2023**, *10*, 2301112. [CrossRef]
52. Kim, J.U.; Park, I.S.; Chan, C.-Y.; Tanaka, M.; Tsuchiya, Y.; Nakanotani, H.; Adachi, C. Nanosecond-time-scale delayed fluorescence molecule for deep-blue OLEDs with small efficiency rolloff. *Nat. Commun.* **2020**, *11*, 1765. [CrossRef]
53. Naveen, K.R.; Lee, H.; Braveenth, R.; Yang, K.J.; Hwang, S.J.; Kwon, J.H. Deep blue diboron embedded multi-resonance thermally activated delayed fluorescence emitters for narrowband organic light emitting diodes. *Chem. Eng. J.* **2022**, *432*, 134381. [CrossRef]
54. Zhang, Z.; Ding, D.; Wei, Y.; Zhang, J.; Han, C.; Xu, H. Excited-state engineering of universal ambipolar hosts for highly efficient blue phosphorescence and thermally activated delayed fluorescence organic light-emitting diodes. *Chem. Eng. J.* **2020**, *382*, 122485. [CrossRef]
55. Zheng, X.; Huang, R.; Zhong, C.; Xie, G.; Ning, W.; Huang, M.; Ni, F.; Dias, F.B.; Yang, C. Achieving 21% external quantum efficiency for nondoped solution-processed sky-blue thermally activated delayed fluorescence OLEDs by means of multi-(donor/acceptor) emitter with through-space/-bond charge transfer. *Adv. Sci.* **2020**, *7*, 1902087. [CrossRef] [PubMed]
56. Zhang, D.; Wada, Y.; Wang, Q.; Dai, H.; Fan, T.; Meng, G.; Wei, J.; Zhang, Y.; Suzuki, K.; Li, G. Highly efficient and stable blue organic light-emitting diodes based on thermally activated delayed fluorophor with donor-void-acceptor motif. *Adv. Sci.* **2022**, *9*, 2106018. [CrossRef]
57. Liang, X.; Tu, Z.L.; Zheng, Y.X. Thermally activated delayed fluorescence materials: Towards realization of high efficiency through strategic small molecular design. *Chem. Eur. J.* **2019**, *25*, 5623–5642. [CrossRef]

58. Cui, L.S.; Gillett, A.J.; Zhang, S.F.; Ye, H.; Liu, Y.; Chen, X.K.; Lin, Z.S.; Evans, E.W.; Myers, W.K.; Ronson, T.K. Fast spin-flip enables efficient and stable organic electroluminescence from charge-transfer states. *Nat. Photonics* **2020**, *14*, 636–642. [CrossRef]
59. Wu, X.; Su, B.K.; Chen, D.G.; Liu, D.; Wu, C.C.; Huang, Z.X.; Lin, T.C.; Wu, C.H.; Zhu, M.; Li, E.Y. The role of host–guest interactions in organic emitters employing MR-TADF. *Nat. Photonics* **2021**, *15*, 780–786. [CrossRef]
60. Park, I.S.; Yang, M.; Shibata, H.; Amanokura, N.; Yasuda, T. Achieving ultimate narrowband and ultrapure blue organic light-emitting diodes based on polycyclo-heteraborin multi-resonance delayed-fluorescence emitters. *Adv. Mater.* **2022**, *34*, 2107951. [CrossRef]
61. Zhang, D.; Song, X.; Gillett, A.J.; Drummond, B.H.; Jones, S.T.E.; Li, G.; He, H.; Cai, M.; Credgington, D.; Duan, L. Efficient and stable deep-blue fluorescent organic light-emitting diodes employing a sensitizer with fast triplet upconversion. *Adv. Mater.* **2020**, *32*, 1908355. [CrossRef]
62. Bian, J.; Chen, S.; Qiu, L.; Tian, R.; Man, Y.; Wang, Y.; Chen, S.; Zhang, J.; Duan, C.; Han, C. Ambipolar self-host functionalization accelerates blue multi-resonance thermally activated delayed fluorescence with internal quantum efficiency of 100%. *Adv. Mater.* **2022**, *34*, 2110547. [CrossRef]
63. Braveenth, R.; Lee, H.; Park, J.D.; Yang, K.J.; Hwang, S.J.; Naveen, K.R.; Lampande, R.; Kwon, J.H. Achieving narrow FWHM and High EQE over 38% in blue OLEDs using rigid heteroatom-based deep blue TADF sensitized host. *Adv. Funct. Mater.* **2021**, *31*, 2105805. [CrossRef]
64. Lee, H.; Braveenth, R.; Muruganantham, S.; Jeon, C.Y.; Lee, H.S.; Kwon, J.H. Efficient pure blue hyperfluorescence devices utilizing quadrupolar donor-acceptor-donor type of thermally activated delayed fluorescence sensitizers. *Nat. Commun.* **2023**, *14*, 419. [CrossRef] [PubMed]
65. Stavrou, K.; Franca, L.G.; Danos, A.; Monkman, A.P. Key requirements for ultraefficient sensitization in hyperfluorescence organic light-emitting diodes. *Nat. Photonic* **2024**, *18*, 554–561. [CrossRef]
66. Ihn, S.G.; Jeong, D.; Kwon, E.S.; Kim, S.; Chung, Y.S.; Sim, M.; Chwae, J.; Koishikawa, Y.; Jeon, S.O.; Kim, J.S. Dipole moment-and molecular orbital-engineered phosphine oxide-free host materials for efficient and stable blue thermally activated delayed fluorescence. *Adv. Sci.* **2022**, *9*, 2102141. [CrossRef]
67. Wright, I.A.; Danos, A.; Montanaro, S.; Batsanov, A.S.; Monkman, A.P.; Bryce, M.R. Conformational dependence of triplet energies in rotationally hindered N-and S-heterocyclic dimers: New design and measurement rules for high triplet energy OLED host materials. *Chem. Eur. J.* **2021**, *27*, 6545–6556. [CrossRef]